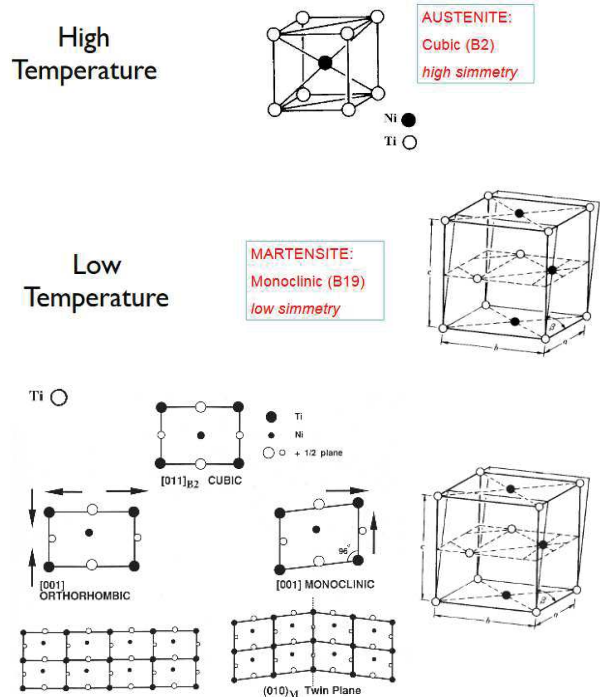


Nanomaterials

Shape memory alloys

A shape-memory alloy is an alloy that "remembers" its original shape and that when deformed returns to its pre-deformed shape when heated.



Nitinol (Ti-Ni) is the most common SMA: it shows a simple cubic austenitic structure at high temperature, whereas at low temperature, the structure becomes monoclinic martensite with low symmetry.

The transformation takes place in different steps: the structure moves from cubic to orthorhombic, then one angle is stretched to less than 90° to obtain the monoclinic structure.

In several crystals, twin planes are formed to accommodate intergranular stresses.

The martensitic transformation is displacive, involving only atom shifts and bond rotations.

It is a fast transformation, occurring at the speed of sound in the material, so there is no time for diffusion.

Monitoring the properties, a hysteresis loop appears: the values of A_s , M_s are determined performing a DSC analysis.

Most shape memory alloys are Ti-Ni (49-51% Ni), but other alloys show this behavior and are employed for high temperature applications or lower mechanical requirements (Cu-Zn).

In Nitinol, the composition is very strict to prevent the precipitation of phases which would decrease detwinning.

The moduli are 80 GPa (austenite) and 40 GPa (martensite), UTS=900MPa as many structural steels, strain at break from 2.5 to 50%.

The matrix constraint forces the grain to maintain its original shape.

To accommodate the large required strain, it may undergo slip or twinning.

Twinning is thermally reversible, obtained by shear stresses, involving only bond rotation.

A mirror plane dividing two symmetric parts defines the twin boundary.

Detwinning permits a considerable deformation without any plane slip.

It is a plastic deformation.

When a threshold stress is reached for martensite, detwinning starts (in a single crystal).

At $T < M_f$, SMA show shape memory effect. The stress-strain curve highlights four main areas.

First, the onset of martensite detwinning until fully detwinned martensite is obtained. Then, detwinned martensite is elastically deformed until the onset of slip and the second deformation until break.

The plateau related to detwinning can reach up to 8%.

The shape memory effect is observed starting from austenite, cooling, deforming martensite, heating and coming back to austenite in the original shape.

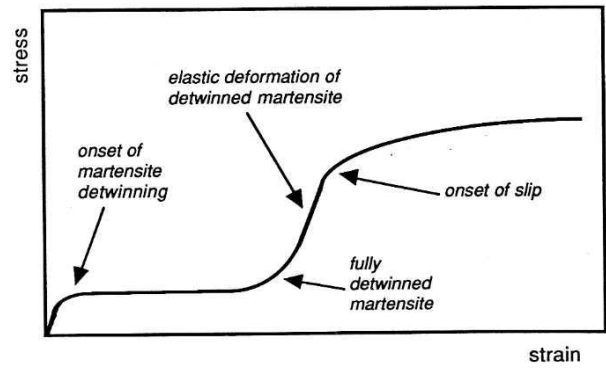
The rotation of cells forces the grains to recover their original shapes.

At $T > A_f$, austenite shows superelasticity. Austenite is elastically deformed and then transformed into martensite, detwinned martensite is elastically and then plastically deformed until break.

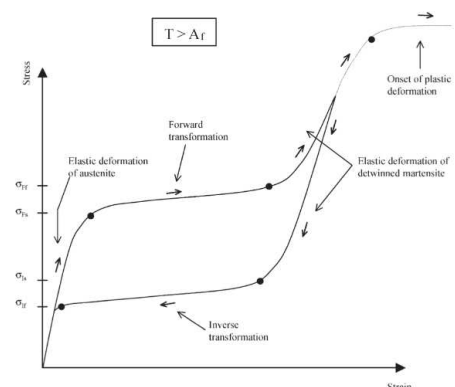
The moduli at $T < M_s$ are the same because the material is martensitic; at $T > A_f$ the stiffness is different because we have the switch between martensite and austenite.

The detwinning plateau is observed to rise with temperature.

If the temperature is too high, the stress required reached the yield stress therefore the deformation becomes plastic, and the material shows no longer shape memory effect.



$T < M_f$



At intermediate temperatures i.e. $A_s < T < A_f$, partial superelasticity is observed, depending on the amount of transformed phase.

There are two kinds of shape memory alloys:

One-way shape memory: heating over A_f , the deformed martensitic phase recovers its original shape.

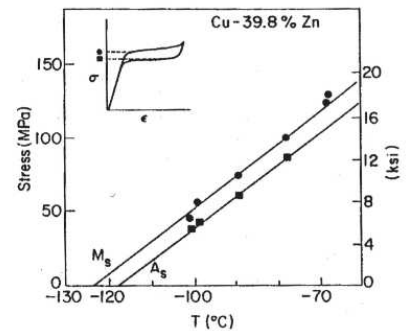
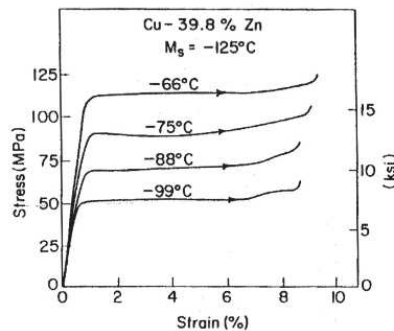
Two-way shape memory: an alloy that has undergone proper training may assume two different shapes at high and low temperature.

The training consists in a thermal-stress cycle where two different shapes are imposed at high and low temperature until the piece stabilizes the two shapes.

This effect is used for actuators that perform a certain work between two different temperatures.

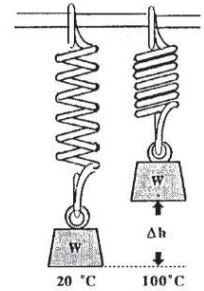
The total number of cycles the piece can perform is limited and depends on maximum deformation, texture, microstructure, composition of the alloy.

The maximum deformation reached is about 1.5%, but it decays with time reaching less than half in 1000 cycles.



SMA Applications

The simplest actuator: at low temperature the weight elongates the spring in the martensite state (lower stiffness), and at high temperature it comes back to austenite recovering its shape.



Actuators in SMA are advantageous because of their simplicity, lightness and they do not require additional components as they substitute both sensor and motor.

They do not undergo problems of wear, sparks, cleanliness and noise, and have high power to weight and volume ratio.

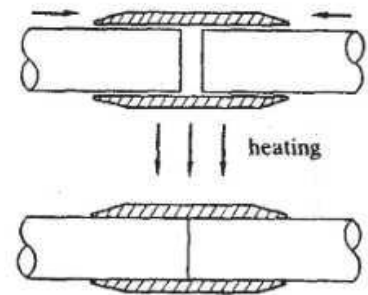
SMA actuators are not energy-efficient, especially with non-uniform load distributions.

They only work with low frequency applications and have a limited number of cycles.

Fasteners, bolt systems and pipe couplings can be produced in SMA for applications with zero insertion force (ZIF).

Thermostatic SMA valves have Nitinol springs which move the spool when the water is too cold or too hot, restricting the flow of water and adjusting the mixture temperature.

One can change the temperature of the mixture from a knob which applies a force to a bias spring.

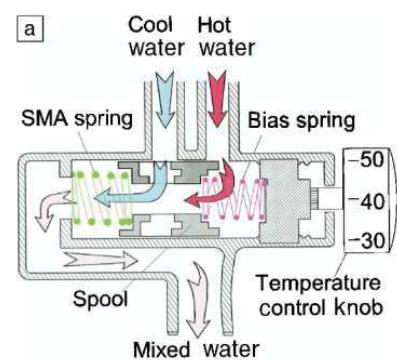


Automatic oil valve adjusting equipment: SMA spring opens and closes the two-way valve unit of automatic oil valve adjusting equipment for gear box according to oil temperature, the volume of oil flow lubricating the pin ion gears is optimized.

This system prevents the oil temperature from rising at the high-speed travelling.

Frangibolts are non-explosive devices which comprises a commercially available bolt and a small collar made of shape memory alloy.

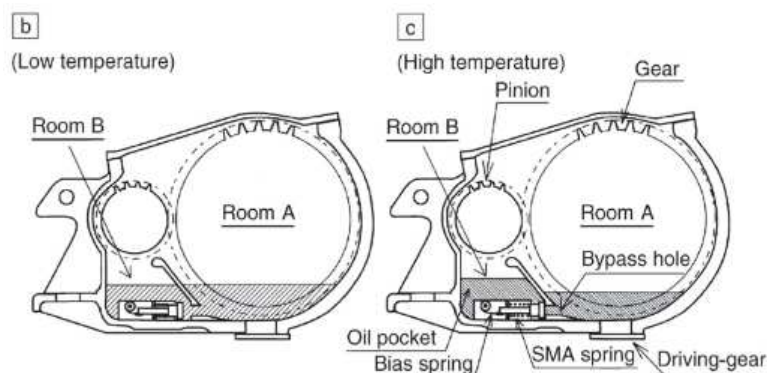
It is a fast actuator which replaces the conventional explosive bolt systems.



Active composites with SMA fibers can be produced.

The matrix is loaded with SMA fibers or wires; if under vibration the element enters resonance, the fibers heat up and transform to austenite introducing a compression in the element and changing its resonance frequency.

Self-repairing materials can be produced as the SMA fibers embedded in the matrix deform on matrix fracture but regain the original shape on heating.



It is possible to use different SMA configurations to customize damping effects. Depending on the temperature, variations are possible on the hysteresis cycle, and the energy dissipation can either be shifted or reduced. At higher frequencies, there is less time to reduce heat, therefore less recovery and less energy is dissipated.

Several biomedical devices are produced exploiting shape memory: orthodontic wires, microsurgery probes, stents etc.

The main applications for SMA are actuators and sensors. For the actuators, one should control the stress-strain curves for the alloy, because shape memory effect works best with high stresses and strain.

The frequency can be the limiting factor for many applications, as there could be no time for recovery.

Magnetic SMA work at higher frequencies as a magnetic field triggers the transformation between austenite and martensite, but lower energies are involved. For higher frequencies and lower strains, piezoelectrics are used.

The main design parameters are transformation temperature, stress rate, suitable recovery force and shape.

Finite elements methods cannot be applied to SMA design, so graphic design is used. One can only design the two extreme points -100% austenite, 100% martensite, as the intermediate behavior is non linear and unpredictable.

The transformation temperature strongly depends on the composition (0.001%), so there is no specific design on temperature: companies select a composition and certify the transformation temperatures for it.

Shape memory ceramics

There are four classes of SMC: viscoelastic, martensitic, ferroelectric, ferromagnetic.

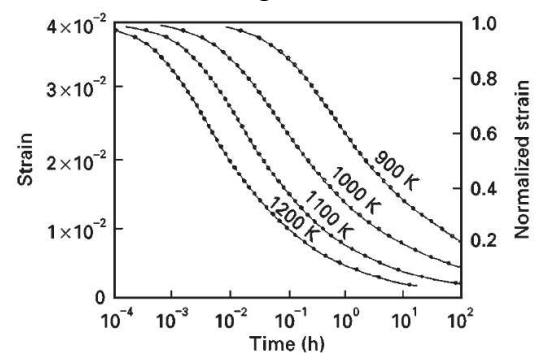
Viscoelastic SMC are mica-based glass-ceramics which can recover up to 0.5% deformation. The process is similar to that of shape memory polymers: plastic deformation at high temperature, cooling down to room temperature to freeze the shape, heating up to high temperature to recover the original shape. The structure consists of 40-60% mica and the remaining is glassy phase. Materials as beta-spodumene are also used.

Mica undergoes plastic deformation by slip of the basal plane over 200 °C. The glass matrix follows the deformation elastically, so that residual stresses are produced. At low temperature, the deformation is retained; increasing the temperature, the mica basal plane can slip under the residual stress from the glass matrix.

Recovery depends on several factors: maximum deformation, temperature, deformation rate, heating time.

The system behaves like a spring + dashpot in parallel.

In general, every ceramic containing a small amount of glass can show SMC behavior, but the deformation recovery is much smaller than in SMA.



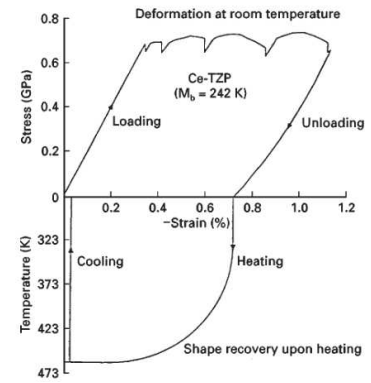
Depending on the temperature, stress relaxation can be observed depending on the temperature.

Martensitic SMC show a behavior similar to that of SMA.

It involves a martensitic transformation of a ZrO_2 based ceramic, or martensitic transformation and re-alignment of ferroelastic domains in some ionic materials ($Pb_3(PO_4)_2$) and superconductors (V-Si).

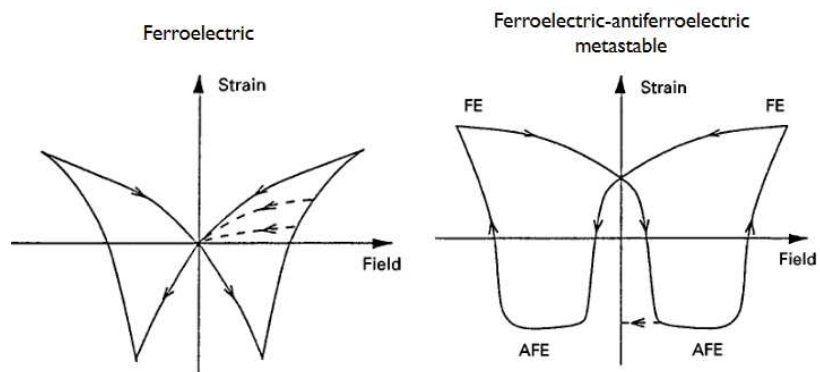
All these materials show both shape memory effect and pseudoelastic deformation.

Stabilized zirconia has no application as every cycle induces cracks.



Ce-TZS shows superelasticity and shape memory effect, with largely different behaviors as temperature changes.

Ferroelectric SMC such as PLZT, PZST, hexagonal manganites as $YMnO_3$ are characterized by the butterfly hysteresis curve. Ferroelectric materials can be polarized by means of the application of an electric field.



Antiferroelectrics have randomly oriented domains.

Applying an electrical field, domains orient more coherently; as the field is stronger, all the domains switch to the direction of the field. In the case of antiferroelectric metastability, one observes a ferroelectric or antiferroelectric phase at zero field depending on the history.

Ferromagnetic SMC are tetragonal manganites or spinels to which detwinning can be imposed by cooling or applying a magnetic field.

As in ferroelectrics, applying a stronger field, martensite can be oriented.

Shape Memory Polymers

Polymers show elastic moduli that range from bakelite to soft rubbers.

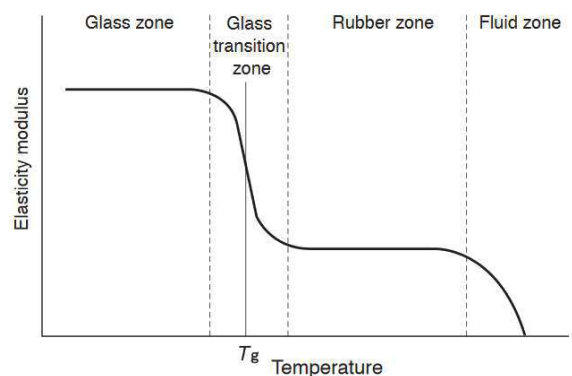
They show a glass transition temperature with an abrupt change of the elasticity modulus. At high temperature they are softer and can be deformed.

Decreasing the temperature below T_g they become rigid but keep the deformed shape.

Returning at high temperature, they recover the original shape.

One can deform the polymer over the T_g up to 200% and freeze the shape below T_g . Heating the polymer over the so-called switching temperature, the polymer without constraints recovers to the original shape if unconstrained.

An unlimited number of cycles can be performed as the elastic component of the viscoelastic system does not change.



SMP allow to control the recovery of different sections of the part by designing the composition of the structure, especially for polymer blends: at the same temperature, a gradient of concentration results in a gradient of shape recovery.

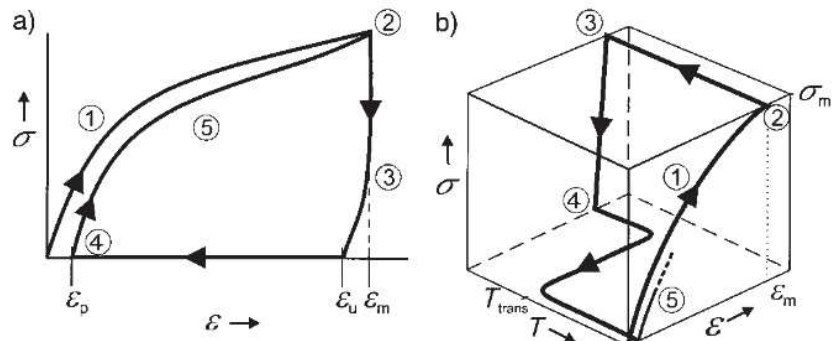
Thermoplastic polymers are normally used, as they are composed of two phases.

One phase has a higher transition temperature T_{perm} that stabilizes the permanent shape like a physical network.

One with lower transition temperature T_{trans} that will work as a switch. $T_{trans} < T_{perm}$, so that SMP deform between the two temperatures.

T_{switch} is the intermediate temperature at which we can deform the material, and it is determined by a thermomechanical test.

The first cycle does not recover completely as the elastic part of the system reaches equilibrium.



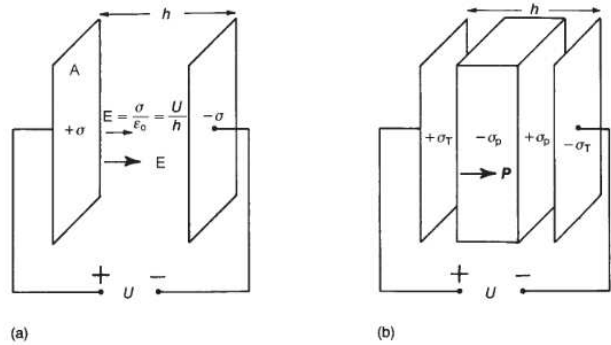
Polarization effect

When an electrical field is applied to a dielectric material there is no long-range transport of charge but only a limited rearrangement such that the dielectric acquires a dipole moment and is polarized. Atomic polarization occurs in all materials: it is a small displacement of electrons around the nucleus. Ionic polarization involves the relative displacement of cation and anion sublattices. Dipolar materials can become polarized as the electrical field orients the molecules.

The most elementary electric dipole comprises two equal and opposite point charges separated by a distance dx . The dipole moment is $p = Q \delta x$.

A polarized material can be regarded as made up of elementary dipolar prisms.

The faces of a prism carry surface energy densities $\sigma_p = \frac{Q}{A}$.



Considering an infinitesimal element, one can define the polarization as the dipole moment per unit volume: $\frac{dp}{dV} = \vec{P} = \sigma_p$. The polarization has the modulus of σ_p and the direction of p .

Considering a parallel plate capacitor with a dielectric between the plates, from Gauss's theorem the electric field is $E = \frac{\sigma}{\epsilon_0}$ between the plates.

The polarization charge density appearing on the surfaces of the dielectric compensates part of the total charge density σ_t , so that $E = \frac{\sigma_t - \sigma_p}{\epsilon_0}$. The electric displacement is $D = \epsilon_0 E + P = \sigma_t$.

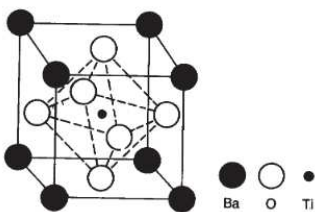
If the dielectric is linear, $P = \gamma \epsilon_0 E$ where γ is the electric susceptibility.

Thus, $D = \epsilon_0 E + \gamma \epsilon_0 E = (1 + \gamma) \epsilon_0 E$.

$$D = \sigma_t = \frac{Q}{A} \rightarrow \frac{Q}{A} = \frac{(1 + \gamma) \epsilon_0 U}{h}$$

$$\text{The capacitance is } C = \frac{Q}{U} = \frac{(1 + \gamma) \epsilon_0 A}{h}$$

The permittivity is $\epsilon = (1 + \gamma) \epsilon_0$, the relative permittivity is $\epsilon_r = \epsilon / \epsilon_0 = 1 + \gamma$.



Barium titanate (BaTiO₃) is the first ceramic material for which ferroelectric behavior was observed.

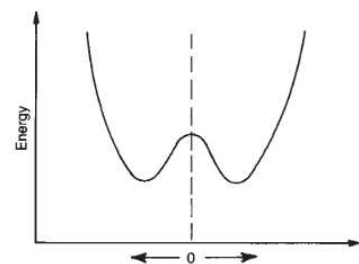
The general perovskite structure is close-packed cubic of ABO₃ with the A ion coordinated with 12 oxygen ions and B ions in the octahedral interstices.

For the perfect fit, the relationship $R_a + R_o = 2t(R_b + R_o)$, where t is a tolerance factor. When $t \neq 1$, small lattice distortions occur to minimize lattice energy and influence the dielectric properties.

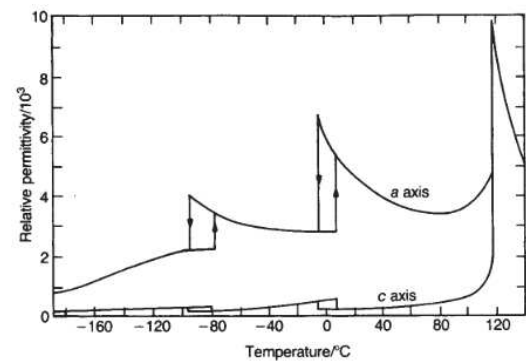
Above its Curie point, $T_c = 130^\circ\text{C}$, the unit cell is cubic.

Below Curie point, the structure is slightly distorted to the tetragonal form with a dipole moment. Below 0°C the unit cell is orthorhombic and below -80°C it is rhombohedral.

Coupling between neighboring columns occurs in BaTiO₃ so that all the Ti⁴⁺ ions are displaced in the same direction. The direction of polarization changes as the crystalline structure changes.



An immediate consequence of the onset of spontaneous polarization in a body is the appearance of an apparent surface charge density and an accompanying depolarizing field. The energy associated with polarization in the depolarizing field is minimized by twinning: the crystal is divided into many oppositely polarized regions (domains) oriented at 180° . This multidomain state can be transformed into a single domain by applying a field parallel to one of the polar directions.



Electrical permittivity changes as the orientation of the domains varies with the temperature and with the crystalline structure.

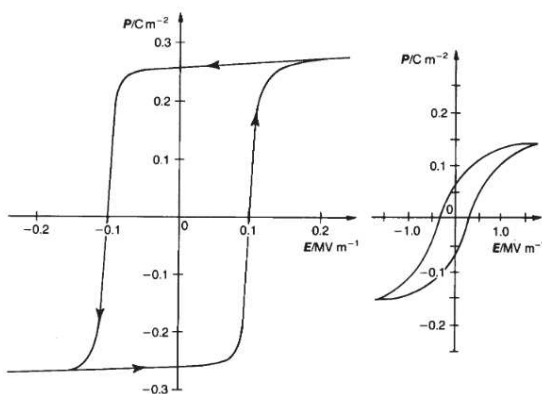
The presence of mechanical stresses in a crystal results in the development of 90° domains to minimize the strain: this configuration can be modified by imposing an electric or mechanical stress.

Ferroelectric ceramics can be transformed into polar materials by applying a static field in a process named “poling”.

Electrostriction: there is no hysteresis cycle and the strain is always negative (striction) if the electric field applied is positive or negative.

In polycrystalline BaTiO_3 the saturation polarization is about half the single-crystal value: in most cases BaTiO_3 is used as a single crystal.

The polarization decreases as the electric field is released because 90° domains are recovered. The field going to the opposite direction will destabilize 90° domains, making them recover and switch to the other direction.



P_r is lower for polycrystalline materials because the 90° domains transform before $E=0$. Critical field E_c is higher for polycrystalline materials because the electrical field must orient both 90° and 180° domains. Ceramic ferroelectrics can have their properties modified by adjusting the composition and the microstructure. Additions and substitution of cations can have different effects: shift Curie T , restrict domain wall motion, introduce compositional heterogeneity, control crystal size, control oxygen

content and Ti oxidation number.

The deformation resulting from the electrical field is displayed in the so-called butterfly curve. Typically, one wants to use piezoelectrics in a restricted domain to make sure that the deformation remains along one direction. By adding Ca to BaTiO_3 , the permittivity broadens close to T_c , so it is easier to have high permittivity far from T_c .

The properties of mixtures of phases depend on the distribution of the components. Any phase in a mixture may be self-connected in 0, 1, 2, 3 dimensions.

The permittivity of a laminate is $\epsilon_z = \sum \epsilon_i \phi_i$, $\epsilon_{x,y} = \sum \epsilon_i^{-1} \phi_i$.

Similarly, for the mechanical properties of composites with long fibers:

$C = \sum \phi C$ is the upper limit (Voigt); $S_c = \sum \phi S$ is the lower limit (Rowes).

Hill performed the average between Voigt and Rowes model, obtaining a more fitting trend.

Lichteneker proposed the best fit: $\log \epsilon = \sum \phi \log \epsilon$.

All materials undergo a small change in dimensions when subjected to an electric field. Some materials develop electric polarization when strained through a stress

Piezoelectric materials have polarization proportional to the stress and the effect is said to be direct.

The strain is also directly proportional to the applied field.

Electrostriction is expressed by the relationship $x = QP^2$ where Q is the electrostriction coefficient.

For materials with $\epsilon_r \gg 1$, $P=D$, $x = QD^2 = Q\epsilon^2 E^2$.

Since most piezoelectrics are ceramics, it is better to load them in compression as they are more resistant that way. In tension we obtain positive electric field, whereas the field is negative under compression.

A polar direction can be developed in a ferroelectric ceramic by applying a static field (poling).

The electrical response due to the direct effect can be expressed as $D=ex$, $E=hx$. The converse effect as $x= g^*D$, $x= d^*E$.

If a biasing field E_b is applied to an electrostrictive material, there will be a direct proportionality between changes in strain and small changes in field: $dx = 2Q\epsilon^2 E dE$ ($E_b \gg dE$).

Ferroelectric materials above their Curie point behave electrostrictively and comparison of the electrostriction coefficient with $\frac{d^*}{2\epsilon P}$ shows them to be of similar magnitude.

The piezoelectric coefficients e , h , g^* , d^* are defined by the partial derivatives

For the direct effect, a constant stress is easier to apply than constant strain, which would require infinite stiffness. Constant electric field is obtained in closed circuit. Thus, the most common conditions are $X=0$ (free from constraints, constant strain), $E=0$ (no electric field, constant).

It can be demonstrated that $d=d^*$, $g=g^*$, $e=e^*$, $h=h^*$.

Assuming these quantities are constant, one can calculate:

$$\frac{d}{g} = \epsilon^X, \text{ permittivity as the stress is } X=0.$$

$$\frac{e}{g} = \epsilon^x, \text{ permittivity as the strain is } x=0.$$

$$\frac{g}{h} = S^D \text{ compliance at open circuit.}$$

The compliance and the stiffness at open and closed circuit are different. When the circuit is closed, $E=0$, the piezoelectric is easier to deform because the domains are free to switch to 90° , so the stiffness decreases. When an electric field is applied, the domains are polarized in the direction of P. the stronger the field, the stronger the polarization, the higher the stiffness.

Equations of state can be written as follows:

$$D = \delta X + \epsilon^X E$$

$$x = S^E X + \delta E$$

$$E = -gX + \frac{D}{\epsilon^X}$$

$$X = S^D X + gD$$

The electromechanical coupling coefficient k is a measure of the ability of a piezoelectric material to transform mechanical energy into electrical energy and vice versa. $k^2 = \frac{W_{12}^2}{W_1 W_2}$

W_{12} : piezoelectric energy density. W_1 : mechanical energy density, W_2 : electrical energy density.

$$W_1 = \frac{1}{2} \delta D \delta E = \frac{1}{2} d \delta X \delta E + \frac{1}{2} \epsilon^X (\delta E)^2$$

$$W_2 = \frac{1}{2} \delta x \delta X = \frac{1}{2} d \delta X \delta E + \frac{1}{2} S^E (\delta X)^2$$

And

thus

simplifying

$$k^2 = \frac{d^2}{S^E \epsilon^X}$$

Equalizing the equations giving dx : $S^E dX + d dE = S^D dX + g dD$, given $\frac{d}{\epsilon^X}$,

$$S^D = S^E \left(1 - \frac{d^2}{S^E \epsilon^X}\right) = S^E (1 - k^2)$$

If $k \ll 1$, $\epsilon^x = \epsilon^X (1 - k^2) \rightarrow k^2 = \frac{\epsilon^X - \epsilon^x}{\epsilon^X} = \frac{[\text{mechanical energy output}]}{[\text{electrical energy input}]}$

The same coupling coefficient works for electrical-to-mechanical and mechanical-to-electrical transformation. To have an efficient piezoelectric, we want low permittivity and compliance. The coupling coefficient is anisotropic, and epsilon is lower along the direction of P.

There are 45 independent tensor components: 21 for the elastic compliance S^E , (4th rank), 6 for the permittivity ϵ^X (2nd rank), 18 for the piezoelectric constant d (3rd rank).

The symmetry of a poled ceramic is described as 6-symmetric or infinite-symmetric.

The constants decrease from 45 to 11:

S: $S_{11} S_{12} S_{13} S_{33} S_{44} S_{66}$

ϵ : $\epsilon_1 = \epsilon_2, \epsilon_3$

D: d_{31}, d_{33}, d_{15} .

There is a correlation between the resonance frequency and the value of k^2 , so the coupling coefficient can be measured.

By the '50s the solid solution system $\text{Pb}(\text{Ti,Zr})\text{O}_3$ which also has the perovskite structure, was found to be ferroelectric and PZT compositions are now most widely exploited of all piezoelectric ceramics.

The phase diagram shows a morphotropic phase boundary at which there is an abrupt structural change, the composition being almost independent of temperature. That is the phase boundary between the high temperature rhombohedral and tetragonal forms is practically a vertical line.

The MPB is a temperature-dependent compositional range over which there is a mixture of tetragonal and monoclinic phases ($0.455 < x < 0.48$).

Phase transformation is the most important phenomenon in PZT for piezoelectric properties transition between tetragonal and rhombohedral.

A polar axis can be conferred on the isotropic ceramic by applying a static field of 1-4 MV/m for several minutes at a temperature above 100 °C. Depoling can be achieved by applying a field in the opposite direction to that used for poling, or in some cases by applying a high AC field and gradually reducing it to zero.

Aging affects many of the properties of piezoelectric ceramics. Most of the piezoelectric coefficients fall by a few % per decade although the frequency constant increases.

Donor dopants (higher charge) are compensated by cation vacancies, acceptors are compensated by oxygen vacancies. Oxygen vacancies are more mobile in perovskite type structures.

Donor doping in PZT would be expected to reduce the concentration of oxygen vacancies, leading to a reduction in the concentration of domain-stabilizing defect pairs and so to lower aging rates. The resulting increase in wall mobility causes the observed increases in permittivity, dielectric losses, elastic compliance and coupling coefficients, and reductions in mechanical Q and coercivity.

Normal powder technology is used in the fabrication of piezoelectric ceramics. The highest values of the coefficients are obtained when the composition is near stoichiometric, the content of fluxing reagents and impurities is minimal, and the density is high as possible. Contamination during milling is kept low by using zirconia-based milling media.

PbO has high vapor pressure, so it evaporates at high temperatures. It must be retained during sintering at temperatures up to 1300 °C. PbO is easily reduced to metallic lead, so all organic constituents must be removed before sintering at about 600 °C in air.

Despite precautions, there is normally a loss of 2-3% of the initial PbO content which is compensated by an addition to the starting materials.

The sintered product usually has a density higher than 95% of theoretical and a crystallite size in the 5-30 um range.

Gas igniter: a force F is quickly applied to generate the voltage, otherwise the voltage generated disappears as charge leaks away through the piezoceramic, across its surfaces and via the apparatus. The magnitude and duration of the applied force must be such that the changes in polarization due to ferroelasticity are reversible if the output of the igniter is not to deteriorate with usage.

Transformers: The regions between the larger electrodes, and between them and the edge electrode, are poled separately. A low A.C. voltage is applied to the larger-area electrodes at a frequency which excites a length mode resonance. A high-voltage output can be taken from the small electrode and the common of the larger ones.

Alternate voltage creates vibrations, so electrical energy is converted to mechanical energy. In the second area, mechanical energy from the vibrations of the first area is converted to electrical energy, producing another alternating voltage.

U_2/U_1 proportional to $h_2/h_1, A_1/A_2$. The ratio U_2/U_1 can reach up to 9000.
$$\frac{U_2}{U_1} = \frac{H_2 A_1}{H_1 A_2}$$

voltage transformers are commonly used in electronic devices. This system can be deposited directly as a coating on the printed circuit board.

Different layers can be stacked to produce a laminate with different parts in parallel at the same voltage. In this way one has several layers with the same voltage and very small thickness.

Accelerometer: during acceleration in the direction of poling the mass exerts a force on the piezoceramic disc and therefore a stress F/A where A is the area of the disc. The measured voltage output is proportional to the acceleration.

Accelerometers have been designed which use ceramics in shear mode. The transducer is a cylinder poled along its axis but with the poling electrodes removed and sensing electrodes applied to the inner and outer major surfaces. The cylinder is cemented to a central post and has a cylindrical mass

cemented to its outer surface. The cylinder is subjected to a shearing action between the mass and the supporting post when accelerated axially.

Actuators: piezoelectric actuators are capable of producing displacements of $10 \pm 0.01 \mu\text{m}$ in a time as short as 10 μs , even when the transducer is subjected to high (100 kgf) opposing forces: these are used for scientific instruments, industrial devices with very small tolerance).

In electrostriction, the sign of the strain is independent of the sense of the electric field. Electrostrictive effect is much smaller than piezoelectric one, but high-permittivity materials can be used just above their Curie point to exploit the effect. Electrostrictive materials do not contain domains, and so return to their original dimensions immediately a field is reduced to zero, and they do not age. The main material is PMN (Mg, Nb).

For a d_{33} value of 500 pm/V, a voltage of 1000 V applied across a 1mm thick poled disc would produce a displacement of only 0.5 μm . Moonie construction is used to magnify displacement. The brass end-caps not only follow the d_{33} -controlled displacement but also redirect the d_{31} displacement into the 3-direction (buckling of the laminae attached to the piezoelectric). This magnified displacement can be as much as 20 μm on a 3mm thick actuator for an applied voltage of as little as 50 V.

Bimorph lamina: Piezoceramics have high stiffness so that large forces are required to generate strains that produce electrical responses. Compliance can be greatly increased by making long thin strips or plates of material and mounting them as cantilevers or diaphragms.

The force F produces a bending moment varying linearly along the length of the beam, being a maximum at the fixed end and zero at the free end. The radius of curvature at a distance l from the fixed end is related to the end deflection by $r = \frac{L^3}{3(L-l)dz}$. This is exploited for reading vinyl records.

The pin moves on the track and oscillates, deforming a double lamina and the deformation is converted into an electrical signal.

MEMS: micro electromechanical systems use surface acoustic waves to make a component move.

Rotary motion is achieved by propagating a SAW round an elastic ring driving a contacting ring slider. Correctly phased vibrations are propagated into the elastic ring from an appropriately poled and energized piezoelectric ring. The SAW is generated by superimposing two standing waves of equal amplitude but differing in phase by $\frac{\pi}{2}$ with respect to both time and space.

Even though the generated force is small, considering that it works at microscale and friction scales with the surface, the force is large enough to allow motion.

Ultrasonic cleaner: for high power ultrasonic applications, transducers are operated at frequencies typically in the range 20-50 kHz. A PZT disc having its fundamental thickness mode frequency in this range would be large, so a composite structure is made with piezoceramic comprised in metal ends. The PZT toroids are kept in compression by the bolt to reduce the risk of their fracturing under the high drive fields.

Tweeter: the active element is a lightly supported circular bimorph. An alternating voltage causes the disc to flex which, in turn, drive a light-weight cone. The frequency response is nearly flat from

about 4 to 30 kHz. The device comprises a poled PZT disc cemented to a thin metal disc which vibrates at the frequency of the applied voltage.

To prevent fracture due to excessive oscillations and resonance at high frequencies, the material is sintered around a steel wire.

Broadband filters: a dielectric body vibrating at a resonant frequency can absorb considerably more energy than at other frequencies provides the basis for piezoelectric wave filters. A filter is required to pass a certain selected frequency band, or to stop a given band. The passband for a piezoelectric device is proportional to k^2 , where k is the appropriate coupling coefficient. Quartz has a very high Q_m which results in a sharp cut-off to the passband. The frequency of quartz oscillators is very well defined (quartz clocks).

Delay line: it can be formed from a slice of an isopaustic glass, designed so that the velocity of sound is as nearly as possible independent of temperature. PZT ceramic transducers are soldered on two 45° metallized edges of the slice. The input transducer converts the electrical signal to a transverse acoustic wave which travels around the device. Epoxy + tungsten powder damping spots clear the unwanted reflections. At the output transducer the signal is reconverted into an electrical signal delayed by the length of time taken to travel around the slice. Such delay lines are used in cathodic tube TV to introduce a delay of approximately 64 μ s, the time taken from the electron beam to travel once across the screen.

Intravascular catheter: an array of 64 PZT bars are arranged around the catheter tip. To form the array a 70 μ m thick poled sheet of PZT is bonded between two metallized polymer sheets. The PZT is sliced into the 64 elements by diamond cutting. The outer polymer film, about 20 μ m thick, serves as acoustic matching layers and carries the thin copper tracks to electrically address each element.

Pyroelectric materials

Pyroelectricity results from the temperature dependence of the spontaneous polarization. Pyroelectricity is shown by all ferroelectric materials. A change in polarization in a solid is accompanied by a change in surface charge and it can be detected by an induced current in an external circuit.

When an electric field is applied to a polar material, the total electric displacement is:

$$D = \epsilon_0 E + (P_s + P_{induced}) = \sigma$$

$\frac{dD}{dT} = \frac{dP_s}{dT} + \frac{Ed\epsilon}{dT}$, where P_s is the spontaneous polarization.

If E is constant, $P_G = P + \frac{Ed\epsilon}{dT}$ is the generalized pyroelectric coefficient.

If the pyroelectric material is perfectly electrically insulated from its surroundings, the surface charges are eventually neutralized by charge flow occurring because of the intrinsic electrical conductivity of the material. Effective neutralization occurs in a time approximately equal to the electrical time constant of the material.

Since pyroelectric materials are polar, they are also piezoelectric, and the strain resulting from thermal expansion will result in the development of a surface charge. However, this is a small effect that seldom exceeds 10% of the primary pyroelectric effect.

Because P_s falls to zero at the Curie point, ferroelectric materials are likely to show high pyroelectric coefficients just below their transition temperatures. High pyroelectric coefficients are observed for ferroelectrics that exhibit second-order transitions such as triglycine sulphate.

Materials which exhibit first-order transition are difficult to exploit because they exhibit hysteresis and in most applications it would be difficult to keep the pyroelectrics in a sufficiently constant temperature environment. A number of materials are used at temperatures well below their Curie points where, although the pyroelectric coefficients are smaller, they vary less with the ambient temperature.

For practical purposes, the very small signals generated by pyroelectrics must be amplified.

Infrared detection

Thin slices of material are coated with conductive electrodes, one of which is a good absorber of the radiation. If radiation at a power density $\frac{W_i}{A}$ is incident on the face for a time dt , the energy absorbed is $\eta W_i dt$. η is the emissivity for the particular surface, wavelength and temperature conditions, and it is also a measure of the fraction of incident energy absorbed.

Assuming that all the power absorbed in time dt is rapidly distributed through the volume of the element, its temperature will rise by dT where $\eta W_i dt = HdT = \rho c_p A h dT$. If part of the absorbed power is lost to the surroundings by reradiation, conduction or convection at a rate G per unit temperature excess $= (T - T_{amb})$, $\eta W_i dt - G T dt = H dT \rightarrow \frac{H dT}{dt} + G T = \eta W_i dt$. If the incident power is shut off at $t=0$, $\frac{H dT}{dt} + G T = 0$, and $T = T_0 \exp\left(-\frac{t}{\tau}\right)$ where $\tau = \frac{H}{G}$ is the thermal time constant.

To obtain a continuous response from a pyroelectric material, the incident radiation is pulsed:

$$\frac{H dT}{dt} + G T = \eta W_0 \exp(j\omega t) \rightarrow T = \left[G\tau \left(\frac{1}{\tau} + j\omega\right)\right]^{-1} \eta W_i$$

The pyrocurrent I_p collected from the electrodes is given by $I_p = \frac{dQ}{dt} = \frac{dT}{dt} \frac{dQ}{dT}$.

$$dQ = AdP = pA \frac{dT}{dt} \text{ in polar state, so } I_p = j\omega \left[G\tau \left(\frac{1}{\tau} + j\omega\right)\right]^{-1} pA\eta W_i$$

The current responsivity is defined as:

$$r = \left| \frac{I_p}{W_i} \right| = \left| j\omega p A \eta (G\tau \left(\frac{1}{\tau} + j\omega \right))^{-1} \right| \rightarrow r = \left| \frac{\omega p A \eta}{G} (1 + \omega^2 \tau^2)^{-1/2} \right|$$

A common arrangement for a detecting system where the voltage u from the pyroelectric element is fed to the gate of an FET (field effect transformer) with a high input impedance. The resistor R_g correctly biases the FET, and C_a and R_a are respectively the input capacitance and resistance of the amplifying and associated system. The voltage output is I_p/Y , where the admittance

$$Y = \frac{1}{R_G} + \frac{1}{R_A} + j\omega(C_E + C_A)$$

[Insert scheme]

C_e is the capacitance of the element. Usually, $R_a \gg R_g$, $C_a \ll C_e$, so $Y = \frac{1}{R_G} + j\omega C_E$ and $Y = \frac{1}{R_G} + (a + \omega^2 \tau^2)^{1/2}$. Where $\tau = R_G C_E$ is the electrical time constant of the circuit.

The voltage responsivity is $r_v = \left| \frac{u}{W_i} \right| = \left| \frac{I_p}{Y W_i} \right| = \frac{r}{|Y|}$.

For maximum sensitivity at low frequency, G should be minimized by isolating the element to reduce the loss of heat. τ can be minimized by reducing the thickness of the detecting element so as to reduce its thermal capacity.

The maximum value of resistivity is $r_{v,max} = \frac{p A \eta R_g}{G(\tau_e + \tau_t)}$.

A figure of merit is introduced, which describes in terms of material properties only, the effectiveness of a pyroelectric element used under define conditions.

$F_V = \frac{p}{c\epsilon}$; the dielectric loss it is $F_d = \frac{p}{c\epsilon^{1/2} \tan^{1/2} \delta}$

PYROELECTRIC MATERIALS

Triglycine sulphate (TGS) has high figures of merit but is a rather fragile water soluble single crystal material. It can be modified to withstand temperatures in excess of its Curie point without depoling, but it cannot be heated in a vacuum to the temperatures necessary for outgassing without decomposing. It is difficult to handle and cannot be used in devices where it would be subjected to either a hard vacuum or high humidity.

Polyvinylidene fluoride (PVDF) has poor figures of merit but is readily available in large areas of thin film, It is considerably more stable to heat, vacuum and moisture than TGS. It is mechanically robust and can have its voltage sensitivity enhanced by the use of a large area. It also has low heat conductivity and low permittivity so that both thermal and electrical coupling between neighboring elements are minimized. Its high $\tan \delta$ is a disadvantage.

[add table]

APPLICATIONS

Pyroelectric materials respond to changes in the intensity of incident radiation and not to a temporally uniform intensity. To obtain a response from stationary objects requires the radiation from them to be periodically interrupted: this is usually achieved by a sector disc rotating in front of the detector and acting as a radiation chopper.

All pyroelectric materials are piezoelectric and therefore develop electric charges in response to external stresses that may interfere with the response to radiation. This can be compensated providing a duplicate of the detecting element that is protected from the radiation by reflecting electrodes or masking, but which is equally exposed to air and mounting vibrations. The duplicate is

connected in series with the detector and with its polarity opposed so that the piezoelectric outputs cancel. This results in a small reduction in sensitivity (<3dB).

[add figure]

RADIOMETRY: the radiant power emitted into a solid angle $d\Omega$ from a small area dA varies with the angle θ measured from the normal to dA : $dW = \frac{\sigma\eta T^4}{\pi} d\Omega dA \cos \theta$. Provided that θ is small,

$$\frac{W}{Ad\Omega} = \frac{\eta\sigma T^4}{\pi}.$$

POLLUTANT CONTROL: the amount of specific impurities in a gas can be monitored by passing radiation from an infrared source through a tube containing a gas sample and then through a narrow passband optical filter corresponding to a frequency at which the pollutant absorbs radiation to a greater extent than any other constituent of the gas (eg. CO₂, CO, NO_x etc. strongly absorb at specific wavelengths).

INTRUDER ALARM: the detector is positioned at the focus of an encircling set of parabolic mirrors. A moving object causes a succession of maxima and minima in the radiation from it reaching the detector. The wavelength λ of radiation emitted with maximum power from a black body at temperature T is given by Wien's displacement law: $\lambda T = 2944 \text{ um K}$. a filter is included which cuts out radiation of wavelengths shorter than about 5 um and so prevents the device from responding to changes in background lighting levels. Such a detector is capable of responding to a moving person up to distances of 100 m.

Electrooptic materials

An electromagnetic wave in the visible part of the spectrum can be emitted when an electron changes its position relative to the rest of an atom, involving a change in dipole moment.

Considering a polycrystalline ceramic with a bias field applied, the symmetry is equivalent to 6mm and the number of tensor components is a minimum.

At $T < T_c$, BaTiO_3 belongs to the tetragonal crystal class (4mm), it is optically uniaxial and the optic axis is the x3 axis.

The form of the electro-optic tensor for 6mm symmetry is identical with that for the 4mm symmetry and the induced birefringence for a field along x3 is $dn = -\frac{1}{2}n^3r_cE$.

For a ceramic to be useful as an electro-optic material it must be transparent. Scattering occurs because of discontinuities in refractive index which usually occur at phase boundaries and pores, and if the major phase is optically anisotropic, at grain boundaries. For transparency, a ceramic should be a single phase fully dense material which is cubic or amorphous (glasses).

The electro-optical properties of dielectrics are determined by their refractive indices or by their permittivities.

In anisotropic dielectric the phase velocity of an electromagnetic wave generally depends on both its polarization and its direction of propagation.

The classical example of an anisotropic crystal is calcite CaCO_3 . Because of the particular arrangement of atoms, light generally propagates at a speed depending on the orientation of its plane of polarization relative to the crystal structure.

For one particular direction, the optic axis, the speed of propagation is independent of the orientation of the plane of polarization.

CaCO_3 is uniaxial, but other crystals can have two optic axes, not necessarily perpendicular.

A linear relationship between P and E is assumed from experiments. The underlying cause is that the largest field strengths commonly encountered in practice are small compared with those that bind electrons in atoms.

The actual response is, however, non-linear. The electro-optic effect has its origins in this non-linearity, and the very large electric fields associated with high-intensity laser light lead to the non-linear optics technology. The permittivity measured for small increments in field depends on the biasing field E_0 from which it follows that the refractive index also depends on E_0 .

The small changes in refractive index caused by the application of an electric field can be described by small changes in the shape, size and orientation of the optical indicatrix. These can be specified by changes in the coefficients of the indicatrix which are assumed to depend on E:

$$\Delta B_{ij} = r_{ijk}E_k + R_{ijkl}E_kE_l = f_{ijk}P_k + g_{ijkl}P_kP_l$$

The constants r, f are the Pockels electro-optic coefficients, and R, g the Kerr coefficients.

$$f_{ijk} = \frac{r_{ijk}}{\epsilon_k - \epsilon_0} \quad g_{ijkl} = \frac{R_{ijkl}}{(\epsilon_k - \epsilon_0)(\epsilon_l - \epsilon_0)}$$

At temperatures below T_c , BaTiO_3 belongs to the tetragonal crystal class; it is optically uniaxial, and the optic axis is the z axis. When an electric field is applied in an arbitrary direction, the representation quadric for the relative impermeability is perturbed to:

$$(B_{ij} + \Delta B_{ij})x_i x_j = 1$$

The main interest is in electro-optical effects in polar ceramic, but generally we speak about materials that change their optical polarization along with their electrical polarization.

A plane wave polarized in z-direction can be written as:

$$\begin{cases} E_x = E_{0x} \sin(k_z z - \omega t) \\ E_y = E_{0y} \sin(k_z z - \omega t + \delta) \end{cases}$$

And this can be also written as:

$$\left(\frac{E_x}{E_{0x}}\right)^2 - \left(\frac{E_y}{E_{0y}}\right)^2 - 2\left(\frac{E_x}{E_{0x}}\right)\left(\frac{E_y}{E_{0y}}\right)\cos\delta = \sin^2\delta, \text{ assuming } z=0.$$

This is the equation of an ellipse, with axes inclined with respect to the x-axis, inclined of an angle depending on the phase angle delta.

- If $\delta = \pi/2$, $\left(\frac{E_x}{E_{0x}}\right)^2 - \left(\frac{E_y}{E_{0y}}\right)^2 = 1$, and if $E_{0x}=E_{0y}$ the ellipse becomes a circle, as major and minor axes coincide with x and y-axes.
- If $\delta = 0$, $\left(\frac{E_x}{E_{0x}}\right)^2 - \left(\frac{E_y}{E_{0y}}\right)^2 - 2\left(\frac{E_x}{E_{0x}}\right)\left(\frac{E_y}{E_{0y}}\right) = 0$, planar polarization is obtained, and we can see many shapes depending on the variation of delta.

Polarizers are polymers with all the fibers oriented along a certain direction, the light output is plane-polarized in the direction of the fibers, perpendicular to the direction of high absorbance.

In polarized light, all the photons have the same phase angle delta.

The propagation speed in a medium depends on its refractive index: $\epsilon_r = n^2$. As ϵ increases, the propagation speed decreases.

Transparent and isotropic materials do not change light polarization once it gets out. If the material has $n_x \neq n_y$, there will be a delay between the two light components and a new δ will be induced ie. polarization change.

Double refraction consists in a partial delay of the light, resulting in two images of the same object. We can modify n_x, n_y, n_z of a crystal if they have different permittivity (anisotropic dielectrics).

In an anisotropic dielectric, the plane velocity of electromagnetic waves generally depends on the polarization of the wave and the direction of propagation.

In an optical axis, the speed of propagation is independent on polarization direction.

$$n_3 = n_2 = n_1 \rightarrow 0 \text{ optical axes} \rightarrow \text{isotropic}$$

$$n_3 \neq n_2 = n_1 \rightarrow 1 \text{ optical axis}$$

$$n_3 \neq n_2 \neq n_1 \rightarrow 2 \text{ optical axes}$$

The impermeability is the opposite of the permeability of a material. $B_{ij} = (\epsilon_R^{-1})$

Under the assumption that the material is non-magnetic, $B_1 = \frac{1}{n_1^2}$ $B_2 = \frac{1}{n_2^2}$ $B_3 = \frac{1}{n_3^2}$

$$\begin{cases} B_1 x_1^2 + B_2 x_2^2 + B_3 x_3^2 = 1 \\ B_i = 1/n_i^2 \end{cases} \rightarrow \frac{x_1^2}{n_1^2} + \frac{x_2^2}{n_2^2} + \frac{x_3^2}{n_3^2} = 1$$

The optical indicatrix is the ellipsoidal surface that represents the plot that n can assume depending on polarization and direction of propagation.

Ordinary rays: the electric displacement component of the wave travels at constant speed irrespective of direction.

Extraordinary rays: the electric displacement component of the wave travels at different speed depending on the polarization direction.

In birefringent materials analysis we assumed ϵ constant, but it is not:

$$D = \epsilon_R E, \text{ and if the material is not magnetic, } \epsilon_z = n^2.$$

We can then assume a trend for the refractive index such that $n = n^2 - AE + BE^2$.

This dependence of n on E is called the electro-optic effect. If the material is centrosymmetric or with a random structure, $A=0$.

B is called Kerr coefficient. Kerr effect is the electric-field optical anisotropy, when $A=0$, typical of non-piezoelectric materials.

If the material is piezoelectric, we can divide mainly linear effect or nevary effect when $A \sim B$:

$$\Delta n \rightarrow \Delta B_{ij} = r_{ijk} E_k + R_{ijkl} E_k E_l = f_{ijk} P_k + g_{ijkl} P_k P_l$$

r, f are electro-optic coefficients, R, g are Kerr coefficients.

Variations of n modify the optical indicatrix.

For linear material like BaTiO₃ at T < T_c with one optical axis, we can evaluate the induced birefringence $\Delta n = n_e - n_o$.

Conversely, if we take BaTiO₃ at T > T_c, it is isotropic i.e. with no optical axis. Applying an electric field, we can create an optical axis and induce optical anisotropy.

$$\Delta n = -\frac{1}{2}n^3(R_{11} - R_{12})E^2$$

A ceramic is useful as an electro-optic material only if it is transparent. Porosity and grain boundaries make the ceramic opaque.

Rayleigh equation: $\frac{I_\theta}{I_0} = \frac{1 + \cos^2 \theta}{x^2} r_p^2 \left(\frac{r_p}{\lambda}\right)^4 \left(\frac{n_p - n_i}{n_p}\right)^2$

For transparency, $I_\theta \rightarrow 0$, therefore a ceramic should be a fully dense single crystal, cubic or amorphous (glass).

- $n_p \sim n$, $\Delta n = 0$, transparent. Little effect on modifying the refractive index, but Kerr effect still is active.
- $\frac{r_p}{\lambda} \rightarrow 0$, very effective way to reduce scattering. This mechanism is also independent from E.

PLZT: PZT + La, highly transparent. Lanthanum substitutes lead and produces different effects on the electro-optical properties. The material has to be homogeneous. PLZT can be obtained pore-free or with grain size below 5 μm by hot pressing. PLZT is often used to control the output of a non polarized light source, since its transparency can be easily tuned.

APPLICATIONS

- Flash goggles: transparent to dark in less than 100 ms, whereas photochromatic glasses take up to 30 seconds. When the sensor detects a flash, the PLZT turns off, decreasing transparency of the whole system up to 1000x. the polarizers are shifted by 90°, blocking most of the light. For normal vision, PLZT is turned on, all the light changes polarization and passes through a second polarizer.
- PLZT display is similar to LCD, we can activate or deactivate a specific pixel with 2 filters and a PLZT in between. It features very fast transition but high operating voltage and current.
- Optical switches: used in optical fibers junction, to keep high speed of laser data transmission. When the PLZT is active, it lets the information pass through; when inactive, it reflects it.

Nanostructured materials

Nanomaterials have at least one dimension in the nanoscale (1-100 nm). Depending on the dimensions in which the size is at nanoscale, they can be classified into:

-nanoparticles, zero dimensionality ie. all dimensions on the nanoscale. These find applications in pharmaceuticals, cosmetics, electronics, optoelectronics (quantum dots) etc.

-layered or lamellar structures have only the thickness at nanoscale. These are used as thin films for electronic devices.

-filamentary structures as nanowires, nanorods and nanotubes have two dimensions at nanoscale

-bulk nanostructured materials consist of large materials made of nanosized crystallites or are amorphous materials. They can possess a nanocrystalline structure or involve the presence of features at the nanoscale.

The higher the dimensionality, the more complex the definition.

A material may be categorized as a nanomaterial simply on the basis of its internal structural dimensions, regardless of its exterior dimensions.

Lamellar structures on nanoscale can be nanocrystalline or microcrystalline: both are defined as nanomaterials. There are typically used as coating, not on their own.

In multilayered structures, each layer can be at nanoscale or above. These result in tougher materials because every layer can arrest failure, yielding very high fracture toughness.

The composition of multilayered nanocoatings can be tailored to reach maximum adhesion and mechanical properties. For example, a TiN coating (better adhesion) on steel with increasing Al composition until pure AlN is reached (higher hardness).

3D bulk nanomaterials exhibit features at the nanoscale such as grain size or precipitates. For example, nanobainitic steels have grain size at nanoscale, precipitation hardened alloys have precipitates at nanoscale.

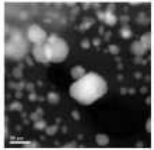
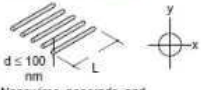
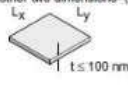
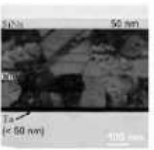
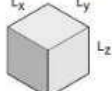
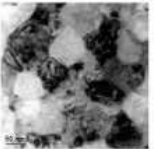
Nanocomposites are formed by two or more materials with very distinctive properties that act synergistically to create properties that cannot be achieved by single materials alone. They can either be composed of a matrix reinforced by nanoparticles, nanowires, nanotubes, or layered structures.

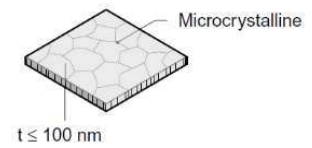
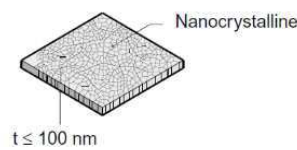
The properties reached can be higher than those predicted by rule of mixtures, but there are many problems related to defect from manufacturing.

Nanocomposites are very hard to sinter, and porosity represents an issue which can hardly be solved.

Being nanomaterials very hard, workability and machinability become very low, and processing becomes very expensive.

Severe plastic deformation can be used to clear the original microstructure and obtain nanoscale features. For example, gold foils can be beaten until nanometric thickness is reached.

Dimensionality	0-D All 3 dimensions on nanoscale	<p>0-D All dimensions (x,y,z) at nanoscale $d \leq 100 \text{ nm}$</p> <p>Nanoparticles</p> <ul style="list-style-type: none"> - amorphous or crystalline - single crystalline or polycrystalline - composed of single or multibranched elements - exhibit various shapes and forms - exist individually or incorporated in a matrix - metallic, ceramic, or polymeric 
	1-D 2 dimensions on nanoscale	<p>1-D Two dimensions (x,y) at nanoscale, other dimension (L) is not</p> <p>$d \leq 100 \text{ nm}$</p> <p>Nanowires, nanorods, and nanotubes</p>  
	2-D 1 dimension on nanoscale	<p>2-D One dimension (t) at nanoscale, other two dimensions (L_x, L_y) are not</p> <p>$t \leq 100 \text{ nm}$</p> <p>Nanocoatings and nanofilms</p>  
	3-D 0 dimensions on nanoscale	<p>3-D No bulk dimension at nanoscale</p> <p>L_x, L_y, L_z</p> <p>Nanocrystalline and nanocomposite materials</p>  



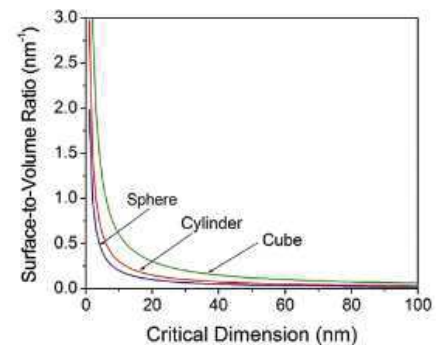
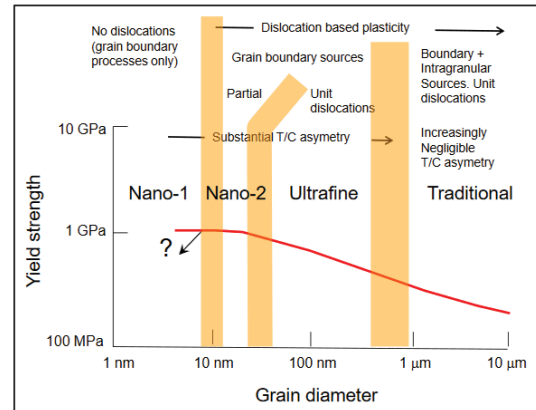
The original definition of nanomaterials is not always appropriate: it is better to refer to a specific size-dependent property that exhibits a critical dimension at nanoscale. For example, the ferromagnetic coercitive force has a critical size at the nanoscale.

The larger surface area/volume of nanomaterials plays an important role in dictating the properties of the material.

The Hall-Petch relationship stops working below about 50 nm. At normal grain size, dislocation movement is the mechanism that justify Hall-Petch relationship. At nanometric grain size, dislocations cannot pile up inside the grains, so dislocation slip is not the mechanism which governs the deformation. Grain boundary sliding is the possible mechanism below a certain grain size.

Ultrafine grain size (100-500 nm) materials show interesting properties and are easier to obtain than nanomaterials.

A nanomaterial's shape is of great interest because various shapes will produce distinct surface-to-volume ratios and therefore different properties. The expressions that follow can be used to calculate the ratios in nanomaterials with different shapes and to illustrate the effects of their diversity.



[MAGIC NUMBERS]

If the energy of each bond is $\epsilon/2$, then for each surface atom not bonded there is an excess internal energy of ϵ/s over that of the atoms in the bulk. In addition, surface atoms will have more freedom to move and thus higher entropy. These two conditions are the origin of the surface free energy of materials.

The surface free energy for a pure material is: $\gamma = E^S - TS^S$.

The geometry of the surface, specifically its local curvature, will cause a change in the system's pressure. These effects are normally called capillarity effects. The curvature of a curve is $k = \frac{1}{r}$. The local curvature is defined positive if the surface is convex and negative if concave.

The Gibbs free energy is given by $\Delta G = \Delta PV = \frac{2\gamma V}{r}$ (Laplace law)

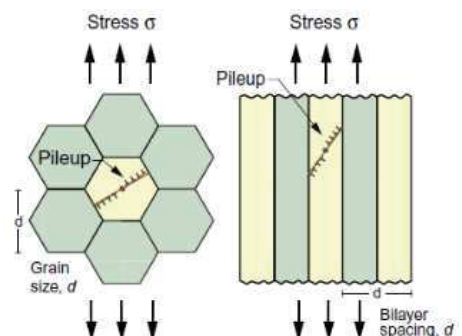
The magnitude of the pressure difference increases as the particle size decreases ie. the local curvature increases.

Hardness increases as the grain size decreases since it is related to the strength of the material.

For normal materials, strength is measured by the force f^* per unit length of dislocation required to cut through the boundary and trigger the slip in the next grain.

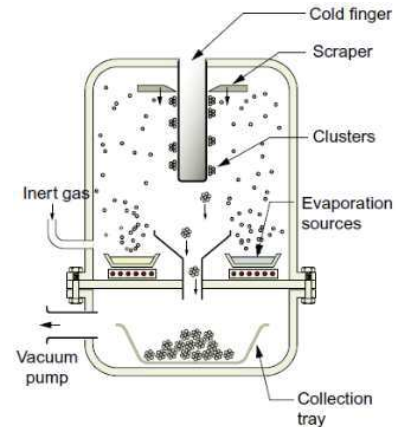
The number of dislocations in a pileup scales with the applied stress and the distance between dislocation source and obstacle.

The smaller the grain size, the lower the number of dislocations N which can pile up. When N falls to 1, no pileup is possible.



Different processing techniques are employed to produced particles, wires, tubes, films or bulk forms.

Inert gas condensation: feed is let evaporate, condensates in a cold finger and falls down to a collector. Once the atoms boil off, they quickly lose their energy by colliding with the inert gas. The vapor cools rapidly and supersaturates to form nanoparticles that collect on a finger cooled by liquid nitrogen. The particles are harvested by scraping them off the finger and are collected, still protected by the inert gas. As particles form they tend to cluster and increase their size.



Sol-gel deposition: a solution of inorganic salts or metal-organic compounds such as alkoxides are polymerized to form a colloidal suspension (sol).

The particles are kept in suspension by adding a surfactant.

The suspension can be treated to extract the particles for further processing or cast onto a substrate.

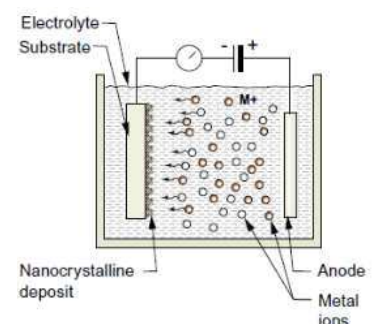
Then it is converted to a gel by chemical treatment to disable the surfactant to create an extended network of connected particles.

Evaporation of the solvent then leaves a dense or nanoporous film.

Pulsed electrodeposition: crystal growth is stopped by pulsing the voltage and adding growth inhibitors that condense on crystal surfaces during the off phase of the pulse.

This technique can yield porosity-free nanocrystalline deposits as thick as 5 mm that require no further processing.

Edge effect is a problem in this technique as a stronger electric field at the corners.

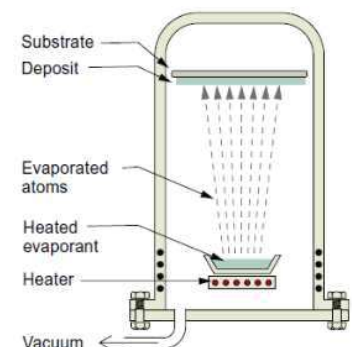


PVD: vapor is created in a vacuum chamber by direct heating or electron beam heating of the metal, from which it condenses onto the cold substrate.

By introducing a reactive gas, compounds can be formed (eg. Sputtering Ti in a nitrogen atmosphere, giving TiN).

Three variants are distinguished:

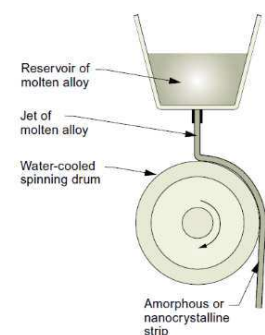
- plating, with no potential difference between bath and workpiece;
- ion plating, the workpiece is the cathode and the source is the anode, so the vapor is accelerated by an electric field;
- sputtering: Ar ions are accelerated onto a target, ejecting ions onto the component surface.
- CVD is similar to PVD, but the reactants are introduced in a vacuum chamber, and the product of the reaction precipitates onto the substrate.



PVD involves temperatures up to 500 °C, whereas CVD requires higher temperatures, up to 900 °C.

Melt spinning consists in casting molten metal onto a rotating wheel, yielding cooling rates up to 10^7 °C/s, giving amorphous or nanocrystalline wires or ribbons.

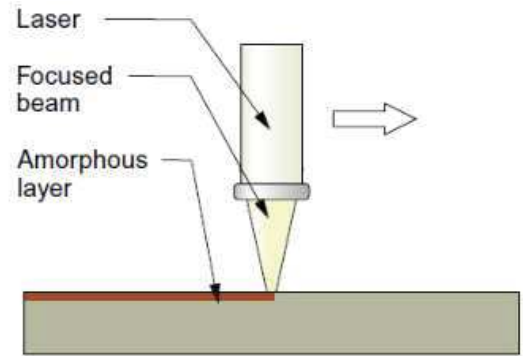
Laser surface hardening consists in melting down a very thin layer of a bulk material, and cooling by conduction is very fast.



Equal channel angular extrusion is the most diffuse severe plastic deformation technique, yielding grain size in the range 200-300 nm.

The resulting parts are very hard and have to be worked by electro discharge machining (EDM).

The major methods of severe plastic deformation are severe plastic torsion straining under high pressure (HPT) and equal channel angular pressing (ECAP)



Electroless deposition involves no electric current. Electroless nickel deposits spontaneously onto almost anything plunged into a bath containing nickel ions and a reducing agent. The deposit is very hard, resistant to wear and corrosion, and cheap.

All powder consolidation processes involve applied pressure.

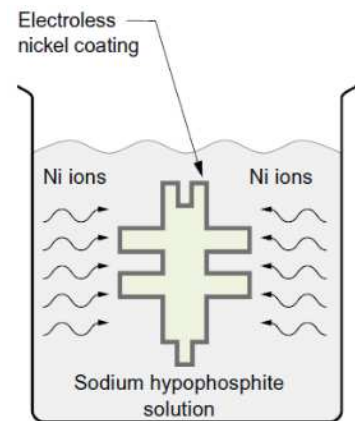
Deformation processes having significant shear stress components are desired:

Extrusion: powders inside a container and pushed through a die

Sinter forging: pressure applied in a hot mold

Uniaxial hot pressing

Hot isostatic pressure: hydrostatic pressure is provided by a gas or a liquid.



The ball milling of powders can be divided into two categories:

- mechanical milling of elemental or compound powders
- mechanical alloying of dissimilar powders in which material transfer occurs.

The minimum grain size obtainable by milling has been attributed to a balance between the defect/dislocation structure introduced by the plastic deformation of milling and its recovery by thermal processes.

Particles are spun in a high energy ball mill. The particles flatten, weld and then break up. The process creates heavily deformed mechanically alloyed particles with a nanoscale internal structure.

Filling the mill with inert gas promotes welding; cryomilling prevents coarsening of the structure.

The particles are subsequently compacter and sintered to make the final product.

In homogeneous mixing between different powders, the particle size reaches a steady state after a certain milling time.

Mechanical alloying is very efficient thanks to the contributions of SPD, temperature and microstructure.

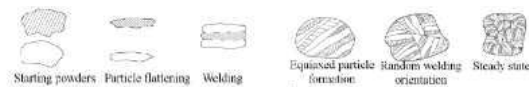
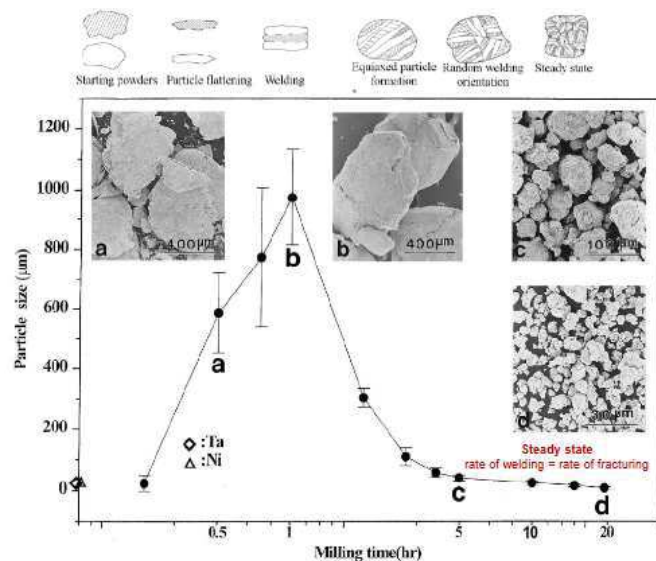
SPD produces crystal defects so that the diffusivity of solute elements into the matrix is enhanced.

Temperature rise increases diffusivity (Arrhenius-like law).

Microstructure refinement decreases diffusion distances.

Type of mill, container, speed, time, grinding medium, ball-to-powder ratio, filling, atmosphere, process control agent, milling temperature are the main parameters influencing the process.

Sintering of metallic powders yields UFG materials.



Nanomaterials: Classes and fundamentals

Currently, the most typical way of classifying nanomaterials is to identify them according to their dimensions. Nanomaterials can be classified as 0-D, 1-D, 2-D and 3-D. This classification is based on the number of dimensions which are not confined to the nanoscale range (<100 nm).

The most common representation of zero-dimensional nanomaterials are nanoparticles. These nanoparticles can be amorphous or crystalline, single crystals or polycrystalline, pure elements or multichemical, exhibit various shapes and forms, exist individually or incorporated in a matrix, be metallic, ceramic or polymeric.

1-D nanomaterials are needle-like shaped like nanotubes, nanorods and nanowires. These can be amorphous or crystalline, single crystal or polycrystals, chemically pure or impure, standalone materials or embedded in within another medium, metallic ceramic or polymeric.

2-D nanomaterials exhibit plate-like shapes like nanofilms, nanolayers, nanocoatings. These can be used as single layer or multilayer, deposited on a substrate, integrated in a surrounding matrix material.

3-D nanomaterials, also known as bulk nanomaterials, are relatively difficult to classify. These materials are thus characterized by having three arbitrarily dimensions above 100 nm. Despite their nanoscale dimensions, these materials possess a nanocrystalline structure or involve the presence of features at the nanoscale.

Bulk nanomaterials can be composed of a multiple arrangement of nanosized crystals, most typically in different orientations. 3-D nanomaterials can contain dispersions of nanoparticles, bundles of nanowires, and nanotubes as well as multi- nanolayers.

A material may be categorized as a nanomaterial simply on the basis of its internal structural dimensions, regardless of its exterior material dimensions.

A 2-D nanomaterial is shown with a particular internal structure, composed of crystals with nanoscale dimension. This can be called a nanocrystalline film because of two features: the material exhibits an overall exterior thickness with nanoscale dimensions, and its internal structure is also at the nanoscale. It is possible for the same film to have a larger (>100 nm) internal grain structure and still qualify the entire material as a nanoscale material.

Generally, 2-D nanomaterials are deposited on a substrate or support with typical dimensions above the nanoscale. In these cases, the overall sample thickness dimensions become a summation of the film's and substrate's thickness. When this occurs, the 2-D nanomaterial can be considered a nanocoating. Yet at times when the substrate thickness does have nanoscale dimensions or when multiple layers with thicknesses at the nanoscale are deposited sequentially, the 2-D nanomaterial can be classified as a multilayer 2-D nanomaterial. Within each layer, the internal structure can be at the nanoscale or above it.

Bulk nanomaterials exhibit features at the nanoscale. When they have crystallites or grains at the nanoscale, they are called nanocrystalline materials.

Another group of 3-D nanomaterials are the so-called nanocomposites. These materials are formed of two or more materials with very distinctive properties that cannot be achieved by each single material alone. Distinctions are based on the types of reinforcing nanomaterials added, such as nanoparticles, nanowires, nanotubes, or nanolayers.

One of the most fundamental differences between nanomaterials and larger-scale materials is that nanoscale materials have an extraordinary ratio of surface area to volume. The properties of large-scale materials are often determined entirely by the properties of their bulk, whereas for nanomaterials the surface-to-volume ratio is inverted. As a result, the larger surface area of nanomaterials plays a larger role in dictating these materials' important properties. This inverted ratio and its effect on nanomaterial properties is a key feature of nanoscience and nanotechnology.

The surface-to-volume ratio of a sphere is given by: $\frac{A}{V} = \frac{4\pi R^2}{\frac{4\pi R^3}{3}} = \frac{3}{R}$.

For a cylinder of radius R, such as a nanowire, the ratio is: $\frac{A}{V} = \frac{2\pi RH}{\pi R^2 H} = \frac{2}{R}$

For a cube of side L, the ratio is: $\frac{A}{V} = \frac{6L^2}{L^3} = \frac{6}{L}$

Eg. Spherical particle of 10 μm to be reduced to a group of particles with 10 nm, assuming that the volume remains constant. One single particle with 10 μm can generate one billion nanosized particles with a diameter of 10 nm, whereas the total volume remains the same. The surface area increases by a factor of 1000.

As the surface-to-volume ratio increases, the fraction of surface atoms increases as the particle size goes down. For a sphere, we can relate the number of surface and bulk atoms according to:

$$V = \frac{4\pi}{3} r_A^3 n, \quad A = 4\pi r_A^2 n^{2/3}$$

Considering a polycrystalline material, in addition to the shape of the particle we have to take into consideration the crystal structure. In FCC structures as Au, Ag, Ni, Al, Cu, Pt, the 14 atoms are all surface atoms.

If another layer of atoms is added so that the crystal structure is maintained, a specific number of atoms must be introduced. In general, for n layers of atoms added, the total number of surface atoms can be given by $N_{total}^S = 2n^2 + 2$, and the total number of bulk atoms can be given by:

$$N_{total}^B = 4n^3 - 6n^2 + 3n - 1$$

These equations relate the number of surface and bulk atoms as a function of the number of layers. These numbers are called structural magic numbers.

From a thermodynamic point of view, the equilibrium shape of nanocrystalline particles is determined by the minimum $\sum A_i \gamma_i$. For ideal FCC metals, the surface energy of atomic planes with high symmetry should follow the order $\{111\} < \{100\} < \{110\}$ due to surface atomic density. On the basis of calculated surface energies, the equilibrium crystal shape can be created. Among the possible shapes, the smallest FCC nanoparticle that can exist is a cubo-octahedron with 14 sides, 12 surface atoms and one bulk atom.

If additional layers of atoms are added to the cubo-octahedral nanoparticle maintaining the same shape and crystal structure, a series of structural magic numbers can be found.

These structural magic numbers do not take into account the electronic structure of the atoms in the nanoparticle. However, sometimes the dominant factor in determining the minimum energy of nanoparticles is the interaction of the valence electrons of the atoms with an averaged molecular potential. In this case, electronic magic numbers, representing special electronic configuration may occur for certain cluster sizes.

SURFACE CURVATURE

The atomic arrangement at the surface is different from that within the bulk. If the energy of each bond is $\frac{\epsilon}{2}$, (energy divided by 2 because each bond is shared by two atoms), then for each surface atom not bonded there is an excess internal energy of $\frac{\epsilon}{2}$ over that of the atoms in the bulk. In addition, surface atoms will have more freedom to move and thus higher entropy. These two conditions are the origin of the surface free energy of materials.

For a pure material, the surface free energy can be expressed as $\gamma = E^S - TS^S$ where E^S is the internal energy, T is the temperature and S^S is the surface thermal entropy.

The geometry of the surface, specifically its local curvature, will cause a change in the system's pressure. These effects are normally called capillarity effects. The radius r is called the radius of curvature at C, whereas the reciprocal of the radius is called the local curvature of the curve at C.

The local curvature is defined as positive if the surface is convex and negative if concave.

Variations in surface curvature will result in changes in the Gibbs free energy given by:

$$\Delta G = \Delta PV = \frac{2\gamma V}{r}$$

The magnitude of the pressure difference increases as the particle size decreases, that is, as the local curvature increases. Therefore, at the nanoscale, this effect is very significant.

The total Gibbs free energy change for the formation of vacancies in a nanoparticle can be expressed as $\Delta G_{total} = \Delta G_{bulk} + \Delta G_{excess}$.

dG_{excess} is the excess Gibbs free energy change for vacancy formation due to curvature effects.

Assuming no surface stress, $dG_{excess} = \frac{\Omega\gamma}{r}$, where Ω is the atomic volume.

The total equilibrium vacancy concentration in a nanoparticle can be given by $X_{tot} = \exp\left(\frac{dG_{tot}}{k_b T}\right)$

For the bulk case, curvature effects can be neglected.

The vacancy concentration under a concave surface is greater than under a flat surface, which in turn is greater than under a convex surface. This behavior has profound consequences on the sintering of nanoparticles. When two nanoparticles are in contact, the neck region between the nanoparticles has a concave surface, which results in reduced pressure. As a consequence, atoms readily migrate from convex to concave surfaces, leading to the coalescence of nanoparticles and elimination of the neck region. Nanoparticles exhibit a high tendency to sintering even at room temperature due to the curvature effect.

The lattice parameter represents the dimensions of the simplest unit of a crystal that is propagated in 3-D, it has significant impact on a variety of properties. To understand the effects of scale on the lattice parameter, we consider the Gauss-Laplace formula: $\Delta P = \frac{4\gamma}{d} = \frac{2\gamma}{r}$.

If the droplet is solid and crystalline with a cubic structure and lattice parameter a , the compressibility of the nanoparticle is $K = \frac{1}{V_o} \left[\frac{\partial V}{\partial P} \right]_T$, which measures the volume change of the material as the pressure applied increases, for a constant temperature. $V_o = a^3$

$$\frac{\gamma}{d} = \frac{3K \Delta a}{4 a}$$

Since the surface energy increases as the particle decreases, because the radius of curvature decreases, the lattice parameter is reduced for a decrease in particle size.

STRAIN CONFINEMENT

Planar defects such as dislocations are also affected when present in a nanoparticle. In the case of an infinite crystal, the strain energy of a perfect edge dislocation loop is given by:

$$W_S = \frac{\mu b^2}{4\pi} \ln\left(\frac{r}{c}\right)$$

Where μ is the shear modulus, b is Burger's vector, r is the radius of the dislocation stress field and c is the core cutoff parameter.

If the crystal size is reduced to the nanometer scale, the dislocation will be increasingly affected by the presence of nearby surfaces. As a consequence, the assumption associated with an infinite crystal size becomes increasingly invalid. Therefore, in the nanoscale regime, it is vital to take into account the effect posed by the nearby free surfaces.

The strain energy of a perfect edge dislocation loop contained in a nanoparticle of size R is given by

$W_S = \frac{\mu b^2}{4\pi} \ln\left(\frac{R-r_d}{R}\right)$ where r_d is the distance between the dislocation line and the surface of the particle. The direct consequence of this behavior is that nanoparticles below a critical size are self-healing as defects generated by any particular process are unstable and ejected.

QUANTUM CONFINEMENT

In bulk crystalline materials, the atomic energy levels spread out into energy bands. The valence band, which is filled with electrons, might be separated from the conduction band by an energy gap. For conductor materials there is typically no band gap, so very little energy is required to bring electrons from the valence band to the conduction band where electrons are free to flow.

For insulator materials the energy band gap is quite significant and thus transferring electrons from the valence band to the conduction band is difficult.

In the case of semiconductor materials, the band gap is not as wide, and thus it is possible to excite the electrons from the valence band to the conduction band with some amount of energy.

This overall behavior of bulk crystalline materials changes when the dimensions are reduced to the nanoscale. For 0-D nanomaterials, where all the dimensions are at the nanoscale, an electron is confined in 3-D space. Therefore, no electron delocalization occurs. For 1-D nanomaterials, electron confinement occurs in 2-D, whereas delocalization takes place along the long axis of the nanowire. In the case of 2-D nanomaterials, the conduction electrons will be confined across the thickness but delocalized in the plane on the sheet.

Therefore, for 0-D nanomaterials the electrons are fully confined. For 3-D nanomaterials the electrons are fully delocalized. In 1-D, 2-D nanomaterials, electron confinement and delocalization coexist.

The effect of confinement on the resulting energy states can be calculated by quantum mechanics as the “particle in the box” problem. The electron is considered to exist inside of an infinitely deep potential well, from which it cannot escape and is confined by the dimensions of the nanostructure. As the energy state E_N is dependent on the dimensionality of the system, so is the number of conduction electrons. This means that the number of electrons dN within a narrow energy range dE , which represents the density of states $D(E) = dN/dE$ is also strongly dependent on the dimensionality of the structure.

The density of states as a function of the energy for conduction electrons will be very different for a quantum dot, quantum wire, quantum well, and bulk material.

Because the density of states determines various properties, the use of nanostructures provides the possibility for tuning these properties: photoemission spectroscopy, specific heat, thermopower, excitons in semiconductors, superconducting energy gap.

Nanomaterials: properties

Most materials are polycrystalline, made up of ordered crystals that meet at boundaries where, inevitably, there is disorder.

Such materials have two structural length scales: that of the crystals and that of the atoms that make them up. Disordered material occupies only a tiny fraction of the volume – less than one part in a million.

Nanocrystalline materials have a greater fraction of disordered material, which now becomes large enough to influence mechanical and other properties.

If the crystal size shrinks further until it becomes of atomic dimensions, the material is now completely disordered. Such materials are called amorphous, meaning without structure. They have only one characteristic length scale, that of the atoms or molecules that make them up.

The amorphous state is the limit of the ultimate nanostructured material, and its properties represent limits.

The bulk properties of materials – density, modulus, yield strength, thermal and electrical conductivity are intrinsic: a small piece of material has the same values for these properties as a large one. It is a basic assumption of continuum mechanics that materials behave in this way, that is, that their mechanical properties are scale independent.

The micromechanical description of materials has assumed that the properties of the individual grains or crystals that make up the material could be averaged to get the overall properties without taking account of their scale. The classical property bounds of solid mechanics rest entirely on this assumption.

As material scientists created higher strength steels and aluminum alloys, it became apparent that the continuum approximation does not always work.

There are many ways to make materials stronger: alloying, dispersion hardening, and work hardening. All are well known and exhaustively studied.

Dispersion hardening as in Al₄Cu alloys is used to obtain nanorods as precipitates which hinder the movement of dislocation and strongly increase the mechanical properties.

Making materials with grains at nanoscale is not easy. The lowest energy state of most materials is as a single crystal. Subdividing it to make it polycrystalline raises its energy because the boundaries where the crystals meet have associated distortions. Therefore, making it nanocrystalline creates a very large area of internal boundary, difficult to make and to retain once made.

MECHANICAL PROPERTIES

The hardness H of copper increases as the grain size is reduced: from 200 MPa to 2000 MPa for 5 nm grain size. $H = \frac{C}{d^{1/2}}$, where C is a constant. This simple dependence must break down at the smallest grain sizes.

The boundaries of grains act as obstacles to dislocation motion, partly because they are locally disordered and partly because the planes on which dislocations glide in one grain are not coplanar with those in the next.

The obstacle's strength is measured by the force f^* per unit length of dislocation required to make it cut through the boundary and trigger a slip in the next grain. This obstacle-like nature of boundaries causes dislocations to pile up against them until the force on the one closest to the boundary exceeds f^* .

The number of dislocation in such a pileup scales with the applied shear stress and the distance L between the dislocation source and the obstacle.

$$N = \frac{\pi L(1 - \nu)(\tau - \tau_0)}{Gb}$$

Where ν is the Poisson's ratio and τ_0 describes the contributions of all the other strengthening mechanisms. The shear stress caused by a tensile or compressive stress σ is $\tau = \sigma/2$.

Since $G = \frac{3E}{8}$, $N = \frac{Cd(\sigma - \sigma_0)}{Eb}$, where C is a dimensionless constant.

The obstacle will be overcome when $N(\tau - \tau_0)b \geq f^*$.

$$\sigma - \sigma_0 = \left(2f^* \frac{E}{Cb}\right)^{\frac{1}{2}} \left(\frac{b}{d}\right)^{\frac{1}{2}} = k^* \left(\frac{b}{d}\right)^{\frac{1}{2}}$$

Where $k^* = \left(\frac{2f^*E}{Cb}\right)^{\frac{1}{2}}$ has the dimensions of stress, and it characterizes the strength of the boundary.

This result is known as the Hall-Petch equation, with k^* the Hall-Petch constant. The hardness is just three times the strength $H = 3\sigma$.

The smaller the grain size d , the fewer the number of dislocations that can be packed into a pileup. The lower is its magnifying effect, the greater is the applied stress needed to break through the obstacle. There comes a point, however, at which N falls to 1 and no pileup is possible. This occurs at a grain size d^* given by $\frac{d^*}{b} < \left(\frac{E}{Ck^*}\right)^2$

Nanolaminates are multilayers, alternating layers, usually of two different materials. The thickness of the layers is between a few atomic layers and a few tens of nanometers. To build a nanolaminate of any thickness then it takes hundreds or thousands of layers.

A nanolaminate made from two soft metals (eg. Cu, Ni) with a bilayer period of a few nm can have a strength of several GPa, putting it within a factor of 2-3 of the theoretical strength of about $E/15$.

As with the nanocrystalline systems, the strength scales as $d^{-1/2}$, where d is now the bilayer period. For deformation to take place, dislocations must sweep through the layers, penetrating the boundaries as they do so. When d is large, pileups form, magnifying the applied stress. The smaller d becomes, the smaller the number of dislocations that can be squeezed into a pileup and the smaller the magnification of the applied stress.

THERMAL PROPERTIES

The melting point of a material is a fundamental point of reference because it directly correlates with the bond strength. For nanoscale solids, for which the ratio of surface to mass is large, the system may be regarded as containing surface phases in addition to the typical volume phases.

For 0-D and 1-D nanomaterials, the curvature of the surface is usually very pronounced. Consequently, for nanomaterials the melting temperature is size dependent.

Surface effects can be expressed mathematically by introducing an additional term to the total energy change resulting from the solid-liquid transformation:

$$\Delta G_{total} = \Delta G_{bulk} + \Delta G_{surface} = \frac{L_0(T_0 - T)}{T_0} V_L + \gamma \Delta A$$

L_0 is the latent heat of melting, T is the melting point of the extended system, V_L is the volume of liquid, γ is the surface tension, ΔA is the increment in surface area.

At the melting temperature, a layer of liquid with thickness t is formed on the surface and moves at a certain rate into the solid. During the change, a new liquid surface and solid/liquid interface are created, whereas the solid surface is destroyed. $\Delta G_{surface} = A_L \gamma_L + A_{SL} \gamma_{SL} - A_S \gamma_S$

L is the new liquid, SL solid/liquid interface, S solid destroyed.

At equilibrium, the solid core of radius r has the same chemical potential as the surrounding liquid layer of thickness t , which occurs when the differential $\frac{\partial \Delta G_{total}}{\partial t} = 0$.

For a sphere, it happens when $\frac{L_0(T_0 - T)}{T_0} = \frac{2\gamma_{SL}}{r - t}$. Assuming $t \rightarrow 0$, which represents the appearance of the first melting, the upper melting temperature for a sphere can be found from the expression $T_M^{upper} = T_0 \left(1 - \frac{2\gamma_{SL}}{L_0 r}\right)$. The upper melting temperature of a spherical nanoparticle decreases with decreasing particle size.

When nanoparticles are embedded in a matrix, the surface of the nanoparticles is in contact with a matrix instead of being exposed to the surrounding atmosphere. The solid/liquid interfacial energy per unit area must be energetically balanced: $\gamma_{LM} - \gamma_{SM} = \gamma_{LS} \cos \theta$

LM: liquid/matrix, SM: solid/matrix, θ wetting angle.

Assuming that $\theta = 90^\circ$, when $\gamma_{SM} > \gamma_{LM}$ the melting temperature of the embedded nanoparticles should be lower than the bulk melting temperature. When $\gamma_{SM} < \gamma_{LM}$, the melting temperature of the embedded nanoparticles should be higher than the bulk melting temperature (superheating).

Due to nanoscale effects, the melting temperature can be either increased or reduced with respect to the bulk material. If the contact angle is lower than 90° , the melting temperature is lower; if the contact angle is higher than 90° , the melting temperature is higher. This is different from the case of standalone nanoparticle, for which the melting temperature always decreases.

$$\begin{aligned} \theta > 90^\circ & \quad T < T_0 \\ \theta < 90^\circ & \quad T > T_0 \end{aligned}$$

Heat is transported in materials by two different mechanisms: lattice vibration waves (phonons) and free electrons. In metals, the electron mechanism of heat transport is significantly more efficient than phonon processes due to the fact that metals possess a high number of free electrons and because electrons are not as easily scattered. In the case of nonmetals, phonons are the main mechanism of thermal transport due to the lack of available free electrons and because phonon scattering is much more efficient. In both metals and nonmetals, as the system length scale is reduced to the nanoscale, there are quantum confinement and classical scattering effects.

In the case of bulk homogeneous solid nonmetals, the wavelength of phonons is much smaller than the length scale of the microstructure. In nanomaterials, the length scale is similar to the wavelength of phonons and thus quantum confinement occurs. Phonon are hindered by quantum confinement only when the nanoparticles become very small.

Free electrons are influenced by band gap quantum effects. Electrons are only slightly affected by scattering at grain boundary. Phonons undergo scattering due to any defect present in the material.

0-D Standalone nanoparticles show quantum confinement. Conductive nanoparticles embedded in a dielectric matrix could yield conductivity in a material thanks to electron tunneling. This occurs when the distance between two nanoparticles is below a certain threshold, so that there is a probability (quantum mechanics) of having electrons passing from one particle to another. The probability of tunneling increases with decreasing distance. The percolation threshold defines the number of particles dispersed in a matrix to have thermal or electrical conductivity. Using nanoparticles, this percolation threshold is very easy to reach with a reduced number of particles.

1-D nanomaterials behave as phonon waveguides similar to optical ones for light. Quantum confinement occurs only on directions at the nanoscale, not along the length of the nanowire. The thermal conductivity of CNT reaches 3000 W/mK, whereas that of Cu is equal to 400 W/mK.

2-D Single-layered nanoscale thin films show that the thermal conductivity is less than those of the corresponding bulk materials. In fact, the thinner the film, the lower the thermal conductivity. In addition, the thermal conductivity of nanofilms increases with increasing temperature, showing the opposite tendency of that in bulk materials. The conductivity increases as the temperature decreases, when the mechanism is dominated by electrons; the conductivity is much lower, and it decreases with temperature when the effect is phonon-dominated. Thermal properties of 2-D nanomaterials are very important for PCs and mobile phones: without vents and with smaller devices, heat must be dissipated very efficiently, so heat transfer must be very efficient.

An interface produces a thermal resistance. This is because an interface constitutes a disruption of the regular crystal lattice on which phonons propagate. The result is that the presence of an interface produces phonon scattering and therefore a reduction in thermal conductivity.

For nano-porous materials, the effect is determined by the number and size of the pores. Due to the porosity, these materials have low permittivity and thermal conductivity. This, in the case of microelectronic components, leads to an increase in the operation temperature and earlier circuit failure. In doped Si polycrystals, the presence of defects increases so phonons are killed. Undoped polycrystals show the lowest conductivity because the grain boundaries affect phonon movement much more than defects introduced by dopants. Doped polycrystals have higher values thanks to the increase in the electron conduction due to dopants.

The heat capacity and coefficient of thermal expansion of nanomaterials have been much less studied. Nanocrystalline Fe was found to have enhanced heat capacity relative to coarse-grained polycrystalline Fe. This effect has been attributed to the entropy contribution to the heat capacity as a result of the large fraction of grain boundaries.

ELECTRICAL PROPERTIES

Electronic conduction at the nanoscale is delocalized, so that electrons can move freely in all dimensions. As the system length scale is reduced to the nanoscale, two effects are of importance:

- Quantum effect, where due to electron confinement the energy bands are replaced by discrete energy states, leading to cases where conducting materials can behave as semiconductors or insulators;
- Classical effect, where the mean-free path for inelastic scattering becomes comparable with the size of the system, leading to a reduction in scattering events.

In 3-D nanomaterials, high grain boundary area-to-volume ratio leads to an increase in electron scattering. Nanosized grains tend to reduce the electrical conductivity.

In 2-D nanomaterials, quantum confinement will occur along the thickness dimension. In fact, as the thickness is reduced to the nanoscale, the wave functions of electrons are limited to very specific values along the cross-section. This is because only electron wavelengths that are multiple integers of the thickness will be allowed and all other wavelengths will be absent. There is a reduction in the number of energy states available for electron conduction along the thickness direction. The electrons become trapped in what is called a potential well of width equal to the thickness.

The effects of confinement on the energy state are: $E_n = \left[\frac{\pi^2 \hbar^2}{2mL^2} \right] n^2$.

For 0-D nanomaterials, the motion of electrons is now totally confined along the three directions. All the energy states are discrete, and no electron delocalization occurs. Under this condition, metallic systems can behave as insulators due to the formation of an energy band gap, which is not allowed in the bulk form.

From a practical point of view, nanomaterials need to be coupled to external circuits by electrodes. For 0-D and 1-D nanomaterials, the contact resistances between nanomaterials and the connecting leads are usually high. One mechanism of providing conduction is through electron tunneling. Electron tunneling is a quantum mechanical effect in which an electron can penetrate a potential barrier higher than the kinetic energy of the electron.

The phenomenon of electron tunneling can be used to develop field-effect transistors (FET) made from quantum dots. Two electrodes, a source and a drain, are coupled to a quantum dot and connected through a circuit. A gate voltage is provided to the quantum dot to control its resistance and the current passing between the lead and drain. Due to the discrete nature of the electrical charge, electrons tunnel from the source to the quantum dot and then to the drain, one at the time.

The junction acts as a capacitor, suffers a raise in voltage when one single electron is added. If the change in voltage is high enough, another electron can be prevented from tunneling (Coulomb blockade). Electrons will not tunnel until a discrete voltage is reached.

In terms of dielectric behavior, the large number of grain boundaries in nanocrystalline materials is expected to increase the dielectric constant. This is due to the fact that under an applied electric field, the positive and negative charges that are segregated at the interfaces will lead to some form of polarization.

In general, for any ferromagnetic material, the total energy can be written as the sum of various terms: $E_{total} = E_{exc} + E_{ani} + E_{dem} + E_{app}$ exchange energy, anisotropic energy, demagnetization energy, energy associated with an applied magnetic field.

This total magnetization energy can be related to a magnetic field according to the expression $E_{total} = MH$ where M is the magnetization vector and H is the applied magnetic field.

Exchange energy is due to the quantum mechanical interaction between atomic magnetic moments and represents the tendency for the magnetization vectors to align in one direction.

The anisotropic energy results from the spin's tendency to align parallel to specific crystallographic axes, called easy axes.

Demagnetization energy is related to the magnetic dipole character of spins, leads to the formation of magnetic domains.

The energy associated with an applied magnetic field is called Zeeman energy, resulting from the tendency of spins to align with a magnetic field. Initially, as the magnetic field increases, the magnetization of the material increases. However, at some point, saturation magnetization is reached, above which an increase in magnetic field does not produce an increase in magnetization. Saturation magnetization is material and temperature dependent.

For nanocrystalline ferromagnetic materials, the exchange forces are dominant due to strong coupling, causing all the spins in neighboring grains to align. There is a critical grain size, below which the material will be single domain. For spherical grains, the critical diameter is: $D_{crit} = \frac{9\gamma_b}{\mu_0 M_s^2}$

If the particle or grain size becomes significantly smaller than the critical diameter, the magnetization is likely to become unstable and loss of magnetization occurs due to thermal fluctuations. These materials are called superparamagnetic.

In bulk ferromagnetic materials, on removal of the magnetic field, the magnetic domains do not revert to their original configuration but there is a remnant magnetization. The coercive field is the applied magnetic field that needs to be applied in the direction opposite to the initial magnetic field to bring magnetization back to zero.

By reducing the particle size or grain size to the nanoscale, the magnetization curve can be altered.

In general, the coercive field of a ferromagnetic material increases with decreasing particle size or grain size, reaching a maximum within a range around the critical diameter.

10-15 nm grain sizes have shown practically no hysteresis: it is possible to produce strong permanent magnets by designing the coercive force to be as high as possible.

Within a specific range of diameters, typically greater than the supermagnetic diameter but lower than the critical diameter, the exchange interaction energy is sufficiently strong to keep the spins aligned during the reversal process. Above this range and below the critical diameter, the process of magnetization reversal becomes incoherent, involving the switching of small volumes of materials within the nanoparticles or nanosized grains.

Magnetoresistance is a material's property whereby the application of a DC magnetic field alters the electrical resistance. Giant magnetoresistance was discovered in films composed of alternating nanoscale layers of ferromagnetic and nonferromagnetic materials. The principle behind this phenomenon is associated with differences in the density of states for spin-up and spin-down electrons in a ferromagnet and the resistance provided by the presence of interfaces.

Conduction electrons with spins parallel to the magnetization will scatter less, whereas electrons with spins aligned opposite to the magnetization will be strongly scattered. If there are two magnetic layers with the magnetization pointing in the same direction, both layers allow electrons in one spin state to pass through, whereas the others will be scattered by each layer.

On the other hand, if the magnetic layers exhibit an antiparallel alignment, both up and down spins will be scattered by each layer, leading to an increase in electrical resistance.

Switching the magnetization of the layers from parallel to antiparallel changes the resistivity from high to low respectively.

To produce an antiparallel magnetization in layered material is not a trivial task.

- Antiferromagnetic coupling involves a nonmagnetic spacer layer with nanoscale thickness between the two ferromagnetic layers. Within a range of spacer thicknesses, the magnetizations of both ferromagnetic layers couple and prefer to lie in an antiparallel state.
- Two ferromagnetic materials with different coercivities can be used: as the magnetic field is reversed, one layer will switch before the other.
- Exchange bias is when a ferromagnetic layer may rotate while a second ferromagnetic layer remains pinned.

Colossal magnetoresistance has been found in certain materials. The resistance can change by orders of magnitude, whereas for giant magnetoresistance it changes around 5%.

If an incident photon has energy greater than the band gap of the material, an electron may be excited from the valence band to the unfilled conduction band. Under these conditions, the photon is absorbed while a hole is left in the valence band when the electron jumps to the conduction band.

At low temperatures, bulk semiconductors often show optical absorption just below the energy gap. This process is associated with the formation of an electron and hole bound to each other, called exciton.

The binding between electron and hole arises from the difference in electrical charge between the electron negative and the hole, leading to a coulombic attractive force across the two particles.

The absorption spectra from excitons can be seen at low temperatures, but they are usually too weak to be observed at room temperature. However, in nanomaterials, as the confinement is enhanced, the exciton binding energy increases, which reduces the possibility for exciton ionization at higher temperatures. As a result, strong excitonic states appear in the absorption spectra of nanomaterials at room temperature.

Optical emission may also occur if the electron and the hole recombine, leading to the generation of a photon. If the photon energy is within 1.8-3.1 eV, the emitted light is in the visible range, a phenomenon called luminescence.

The smaller the nanoparticle size, the shorter the wavelength of the visible light that's emitted.

The shift from the blue to the red corresponds to an increase in nanoparticle size. An issue of importance is the use of a homogeneous distribution of nanoparticles, because fluctuations in size and composition can lead to an inhomogeneous spreading of the optical spectra.

The optical properties of metallic nanomaterials are also affected by nanoscale.

Gold has a yellow color in bulk form, whereas Au nanoparticles give ruby-red, purple, or even blue color depending on the size.

Plasmons are quantized waves propagating in materials through a collection of mobile electrons that are generated when a large number of these electrons are altered from their equilibrium positions. Plasmons are observed in Au, Cu, Ag, Mg, Al.

Surface plasmons have lower frequencies than bulk plasmons and thus can interact with photons. In fact, when photons couple with surface plasmons (producing polaritons), alternating regions of positive and negative charges are produced in the surface of the material, thereby generating an electrical field of plasmons.

Surface plasmon polaritons cannot be produced on smooth metal surfaces in contact with air, mainly because the momentum of light is different from the momentum of surface plasmons. To cause a change in momentum, a thin layer of metal is placed between two materials with different refractive indices. If the angle of the incidence light on the material with higher refractive index exceeds a critical angle, evanescent waves can propagate surface-plasmon polaritons along the metal layer.

Another technique to induce surface-plasmon polaritons is to roughen the material's surface. This can be done by creating parallel linear features on the surface of the material or by randomly roughening the surface.

When the refractive index or dielectric constant of the material embedding the nanoparticles increases, the plasmon frequency decreases, generating a red shift.

Acoustic waves, which exhibit wavelengths that range from microns to kilometers, have little to no direct effect on the properties of nanomaterials. As a result, the discussion of acoustic properties is limited for the case of nanomaterials. However, it should be pointed out that sound waves are used to produce nanomaterials.

Carbon nanotubes are cylindrical molecules with a diameter of few nanometers and length up to a few micrometers. Their structure consists of a graphite sheet wrapped into a cylinder.

Depending on the processing conditions, CNTs can be either single walled or multiwalled.

Single-walled nanotubes may be metallic or semiconductor, depending on the orientation of the hexagonal network with respect to the nanotube long axis (chirality).

CNTs can be classified by a chiral vector given by $c = na + mb$, where a and b are unit vectors and n , m are chiral vector numbers that characterize the orientation of the hexagons in a corresponding graphene sheet.

The magnitude of the chiral vector is the circumference of the nanotube, and its direction relative to the unit vector a is the chiral angle.

Carbon nanotubes can have different structures: armchair, zigzag, or chiral.

An armchair nanotube is formed when $n=m$. the zigzag nanotube forms when $m=0$. The chiral type occurs when the chiral vector numbers can assume any integer values and the chiral angle is intermediate between 0 - 30° .

So far, researchers around the world have been devising several methodologies to synthesize CNTs. The most common methods are the arc-discharge technique and the chemical vapor deposition. These methods have seen significant improvements over the years, but still they suffer from low yield, very high cost, difficulty in tuning the diameter of the nanotubes, and difficulty in producing a single type of CNT without impurities.

Due to their outstanding properties, CNTs are likely to play a vital role in various areas, such as nanocomposites, nanoelectronics, hydrogen storage, field emission devices, and nanosensors.

Nanomaterials: synthesis and characterization

0-D

Nanoclusters are made by gas-phase or liquid-phase processes.

The most common gas-phase processes are gas inert condensation and inert-gas expansion.

Liquid phase processes use surface forces to create nanoscale particles and structures. There are several processes such as ultrasonic dispersion, sol-gel methods, and methods relying on self-assembly.

In inert-gas condensation, an inorganic material is vaporized inside a vacuum chamber into which an inert gas is periodically admitted. The source of vapor can be an evaporation boat, a sputtering target, or a laser-ablation target. Once the atoms boil off, they quickly lose their energy by colliding with the inert gas. The vapor cools rapidly and supersaturates to form nanoparticles with sizes in the range 2-100 nm that collect on a finger cooled by liquid nitrogen. The particles are harvested by scraping them off the finger and are collected, still protected by inert gas, for further processing. Alloy particles are made using dual sources. The problem with this method is that as the particles form, they tend to cluster and increase their size.

In inert-gas expansion, evaporated atoms are carried by a high-pressure helium gas stream that is expanded from a nozzle into a low-pressure chamber at supersonic velocities. The adiabatic expansion of the gas leads to sudden cooling, causing the evaporated atoms to form clusters a few nanometers in diameter.

Sonochemical processing involves ultrasounds to nucleate a chemical reaction. A magnetostrictive or piezoelectric transducer is used to generate ultrasonic waves with a wavelength of 1-10000 microns in a liquid-filled reaction vessel. These are not molecular dimensions, so there is no direct coupling of the acoustic field with the chemical species.

The reaction occurs because of cavitation. The tensile part of the wave is intense enough to pull the liquid apart and form a tiny cavity. Reactants are vaporized inside it, then the compression part of the wave then compresses it. The next tensile wave re-expands the bubble, which oscillates in volume at the frequency of the sound waves, pumping it up as more vapor enters during the expansion part of the cycle. When the bubble reaches a critical size, it collapses. The collapse is adiabatic because the very fast collapse rate leaves no time for heat flow, generating a tiny localized hot spot. Temperatures and pressures are very high (up to 5000°C, 2000 atm), triggering reactions that create a nanoparticle within the spot. The size of the spot determines the size of the resulting particles. By using organometallic precursors, ceramic and metallic particles as small as 2 nm can be produced. The technique can be used to produce a large volume of material for industrial applications.

Ultrafine particles, nanothickness films, and nanoporous membranes can be made by sol-gel processing.

The precursors are usually inorganic metal salts and metal-organic compounds such as alkoxides and metal ions with an organic ligand.

Polymerization reaction forms colloidal suspensions of discrete, finely dispersed particles kept in suspension by adding a surfactant. The suspension can be treated to extract the particles for further processing, or it can be cast or spin-coated onto a substrate. There it is converted to a gel by chemical treatment to disable the surfactant to create an extended network of connected particles. Evaporation of the solvent then leaves a dense or nanoporous films.

Molecular self-assembly methods rely on the self-organization of organic molecules. The most obvious is that of crystallization. The idea is to create the conditions under which atoms or

molecules will self-assemble into useful structures, driven by the minimization of their energy. The system converges to a specific configuration without the need for further control.

The self-assembly of molecules form micelles. Micelles are aggregates of amphiphilic molecules (one end is hydrophobic, the other is hydrophilic). These aggregates form spontaneously at a size that depends on the concentration of amphiphilic molecules in solution. The center of the micelles act as a chamber for chemical reactions and thus dictates the size of the created nanoparticle. Typically the aggregates formed are bonded by relatively weak bonds.

Self-assembly of 2-D nanofilms is made possible by using the Langmuir-Blodgett technique. A monolayer of a fatty acid is created on the surface of water into which a substrate has been placed. The fatty acid self-spreads across the water surface as a monolayer. The substrate is slowly withdrawn from the water, and the monolayer sticks to it and is transferred from the water surface to the substrate. The process allows the fabrication of single monolayers of materials as well as thicker films by repeatedly dipping and withdrawal.

1-D

The production route for rodlike nanomaterials by liquid-phase methods is similar to that for the production of nanoparticles.

Self-assembly methods use the highly anisotropic bonding nature of asymmetric molecules to cause them to self-assemble into tubes rather than spheres, forming cylindrical micelles. The amphiphilic molecules are then removed with an appropriate solvent or by calcining to obtain individual nanowires.

CVD methods have been adapted to make 1-D nanotubes. Catalyst nanoparticles are used to promote nucleation. To make carbon nanotubes, for example, a combination of carbon-containing gases such as methane are reacted in the presence of Fe, Co, and Ni catalysts at 1100 °C. decomposition of the gases releases free carbon atoms that condense on the substrate with its array of catalyst particles, from which the carbon nanotubes grow.

Nanowires of other materials such as Si, Ge are grown by vapor-liquid-solid methods. A catalyst seed is deposited on a substrate. A vapor phase with the desired composition is brought in contact with the seed at a controlled temperature. The vapor diffuses into the catalyst, changing its composition and lowering its melting point until it melts. The liquid surface acts as a preferred site for absorption of the vapor. The liquid becomes supersaturated and a solid nanowire or whisker then grows from it with a diameter equal to the diameter of the catalyst seed.

Foil beating is achieved by beating the metal to a uniformly thin foils, roughly 100 nm thick. In gilding, it is applied by smoothing it onto the adhesive coated surface of the object to be gilded.

Electrodeposition is a long-established way to deposit metal layers on a conducting substrate. Ions in solution, sometimes replenished from an anode, are deposited onto the negatively charged cathode, carrying charge at a rate that is measured as a current in the external circuit. The process is relatively cheap and allows complex shapes. The layer thickness simply depends on the current density and the time for which the current flows.

The challenge is to control the structure. Most electrodeposits grow in a columnar manner. To make nanoparticles or layers, it is necessary to stop each crystal growth while it is still tiny and to nucleate more. By adding a pulsating voltage and growth inhibitors, these condense on the crystal surfaces during the “off” phase of the pulse and prevents growth during the “on” phase.

This technique can yield porosity-free nanocrystalline deposits as thick as 5 nm that require no further processing.

In PVD plating, a thin layer of a material is deposited from a vapor onto the object to be coated. The vapor is created in a vacuum chamber by direct heating or electron beam heating of the metal, from which it condenses onto the cold substrate.

In PVD ion plating the vapor is ionized and accelerated by an electric field.

In PVD sputtering, Ar ions are accelerated by the electric field onto a metal target, ejecting ions onto the component surface.

Almost any metal or compound that does not decompose chemically can be sputtered.

In CVD processing, a reactant gas mixture is brought into contact with the surfaces to be coated, where it decomposes, depositing a dense pure layer of a metal or compound. The deposit can be formed by a reaction between a vapor and the surface of the substrate itself. A difficulty with the process is that it frequently requires temperatures above 800 °C.

In moderate temperature CVD, metal organic precursors are used, as they decompose at relatively lower temperature. If the chemical reactions in the vapor phase are activated by the creation of a plasma in the gas phase (plasma-assisted CVD) or by shining a laser beam into the gas mixture (laser CVD), deposition at an even lower temperature becomes possible.

There are three directions of attack to produce bulk nanomaterials. The top-down approach breaks down the structure of a bulk material, reducing the crystal size to submicron or nano-dimensions.

The intermediate approach is milling micro particles to reduce their structure to the nanoscale. The bottom-up approach involves building up from the atomic scale or nanoclusters to retain the scale of its structural units.